Chapter 5

Carbon Dioxide Fluxes in the Global Ocean

Andrew J. Watson · James C. Orr[1]

5.1 Introduction

Atmospheric carbon dioxide concentration is one of the key variables of the 'Earth system' – the web of interactions between the atmosphere, oceans, soils and living things that determines conditions at the Earth surface. Atmospheric CO_2 plays several roles in this system. For example, it is the carbon source for nearly all terrestrial green plants, and the source of carbonic acid to weather rocks. It is also an important greenhouse gas, with a central role to play in modulating the climate of the planet. During the five thousand years prior to the industrial revolution, we know (from measurements of air trapped in firn ice and ice cores) that atmospheric CO_2 varied globally by less than 10 ppm from a concentration of 280 ppm (Indermuhle et al. 1999). During the late Quaternary glaciations, the regular advance and retreat of the ice was accompanied by, and to some extent at least driven by (Li et al. 1998; Shackleton 2000), an oscillation in atmospheric CO_2 of about 80 ppm. Evidence from the geologically recent past indicates, therefore, that quite small changes in atmospheric carbon dioxide have big effects on planetary climate. Conversely, a stable concentration of CO_2 is necessary for a stable climate. By this reasoning, we can be fairly certain that human activities will have a major effect on the climate of the planet in the near future, given that we have raised CO_2 by 90 ppm in the last 150 years and it is projected to double from the pre-industrial concentration during the coming century. This gives our investigations into sources and sinks of carbon dioxide a special urgency.

For reasons that are made clear below, the oceans occupy a central role in the global carbon cycle and the processes influencing the concentration of CO_2 in the atmosphere. The JGOFS program represented the first sustained global effort to document the present state of the oceanic carbon cycle, and to test our understanding by comparing that state with the predictions of increasingly sophisticated numerical models. In the subsequent sections, we first discuss the role of the oceans in setting global atmospheric CO_2. JGOFS has made a major contribution to our estimate of the size of the present net flux of CO_2 from atmosphere to ocean, and we next review our estimates of this 'sink' and how it may change in the future. This leads us to a discussion of the advances made in understanding the processes involved in setting that flux. Finally we summarize what we have learned during JGOFS and what the major topics of research are likely to be in the next 10 years.

5.2 The Oceans' Influence on Atmospheric CO_2

In this section, we review some basic facts and figures about the oceanic component of the carbon cycle. Some of this knowledge was well established prior to JGOFS, but much of the detail is recent, and comes from JGOFS and related activities.

5.2.1 The Ocean Sets the Steady-State Atmospheric CO_2 Concentration

Figure 5.1, modified from Houghton et al. (1990) and Watson and Liss (1998), is a summary of the global carbon cycle in reservoir-flux form. One-way fluxes between the atmosphere and ocean are about 70 Pg C yr^{-1}, of the same order as the exchange between the atmosphere and the terrestrial biota. The present sink for atmospheric CO_2 in the oceans is the net imbalance between the ingoing and outgoing fluxes and is of order 2 Pg C yr^{-1}, just ~2% of the one-way fluxes. This net uptake has occurred as a response to increasing CO_2 in the atmosphere. In the pre-industrial era the oceans were a small net source to the atmosphere, as explained below in the section on 'The Pre-Industrial Steady State'.

[1] Ocean carbon model intercomparison results were contributed by the following authors: O. Aumont, K. G. Caldeira, J.-M. Campin, S. C. Doney, H. Drange, M. J. Follows, Y. Gao, A. Gnanadesikan, N. Gruber, A. Ishida, F. Joos, R. M. Key, K. Lindsay, F. Louanchi, E. Maier-Reimer, R. J. Matear, P. Monfray, A. Mouchet, R. G. Najjar, G.-K. Plattner, C. L. Sabine, J. L. Sarmiento, R. Schlitzer, R. D. Slater, I. Totterdell, M.-F. Weirig, M. E. Wickett, Y. Yamanaka and A. Yool.

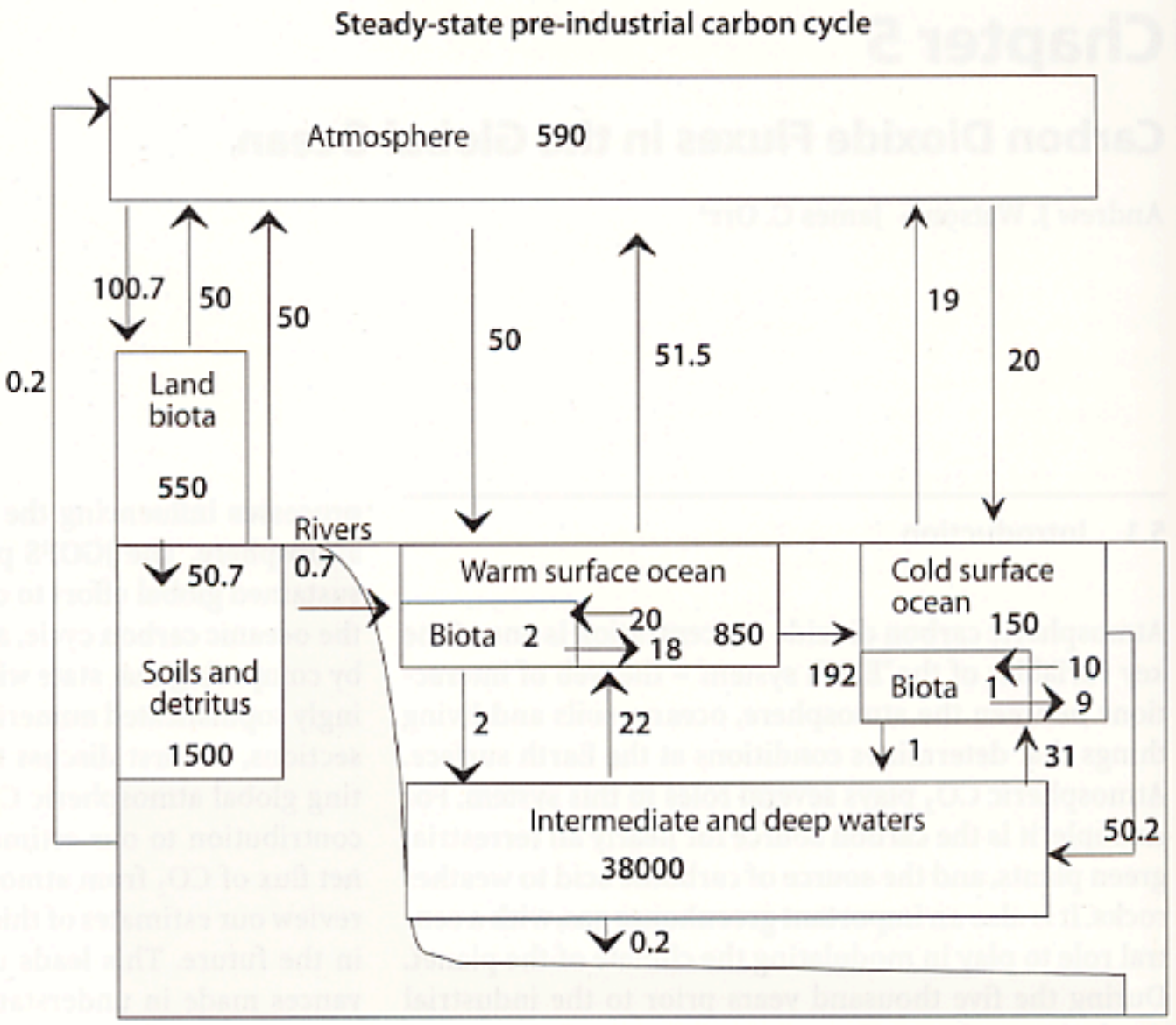

Fig. 5.1.
Reservoir-flux representation of the steady-state, pre-industrial global carbon cycle. Reservoir sizes are in Pg C, and fluxes in Pg C yr^{-1} (1 Pg = one petagram ≡ 1 Gt = one gigatonne = 10^9 tonnes). The figure is adapted from Houghton et al. (1990) with additional information from Sarmiento and Sundquist (1992), Sarmiento and Toggweiler (1984) and Sundquist (1985). Fluxes are adjusted so that the net flux into each reservoir is zero, which sometimes involves specifying fluxes to a higher accuracy than that to which they are in reality known

As the figure shows, most of the carbon that is not locked up in carbonate rocks resides in the ocean, which contains 15–20 times as much carbon as the atmosphere, land vegetation and soils combined. About 90% of the carbon in the ocean is in the form of bicarbonate ion, mostly in the deep sea. The atmosphere exchanges CO_2 rapidly with both the ocean surface and with the land vegetation, such that the residence time of a CO_2 molecule in the atmosphere is only about 10 years with respect to these reservoirs.

The 'one-way' fluxes between ocean and atmosphere are proportional to the partial pressures of CO_2 in the atmosphere and at the ocean surface. (Strictly we should use fugacity rather than partial pressure, to account for the slight departure from ideal gas behaviour of CO_2. In practice, the difference is about 1%. We have chosen to ignore it to make the discussion more accessible to non-chemists who may understand the concept of partial pressure but be unfamiliar with fugacity.)

$$F_{\text{air}\rightarrow\text{sea}} = KpCO_{2\text{air}} \qquad (5.1)$$
$$F_{\text{sea}\rightarrow\text{air}} = KpCO_{2\text{sea}}$$

where the constant of proportionality is K, the CO_2 gas exchange coefficient (and is a 'constant' only in the sense that it is independent of CO_2 concentrations). Since the ingoing and outgoing fluxes balance within 2% when integrated over the ocean surface as a whole and periods of a year, (and provided variations in K do not correlate with variations in pCO_2),

$$\overline{\overline{pCO_{2\text{air}}}} \approx \overline{\overline{pCO_{2\text{sea}}}}$$

where the double overbars represent the time and area averages. If some disturbance were to force atmospheric CO_2 away from near-equilibrium with the ocean, the resulting imbalance of fluxes across the air-sea interface would, on a time scale of a decade, tend to adjust atmospheric and sea surface CO_2 until the steady state was re-established. On a time scale of many centuries, when steady state was restored between deep ocean and the surface, any anomaly in CO_2 would be diluted into the large deep ocean reservoir, so that the final departure from the original steady state would be comparatively small. However, altering the parameters that set the partial pressure of CO_2 at the sea surface, such as the amount of biologically driven flux out of the surface layers or the temperature of the sea surface, will have a direct effect on the steady-state CO_2 content of the atmosphere, within a few decades.

Examples of this behaviour are given in Fig. 5.2a and b using calculations from a very simple box model of the ocean and atmosphere (Sarmiento and Toggweiler 1984), and ignoring changes in the land vegetation and interaction with the sediments. Figure 5.2a shows the result of disturbing the system by an exponentially increasing release of CO_2 into the atmosphere, similar to

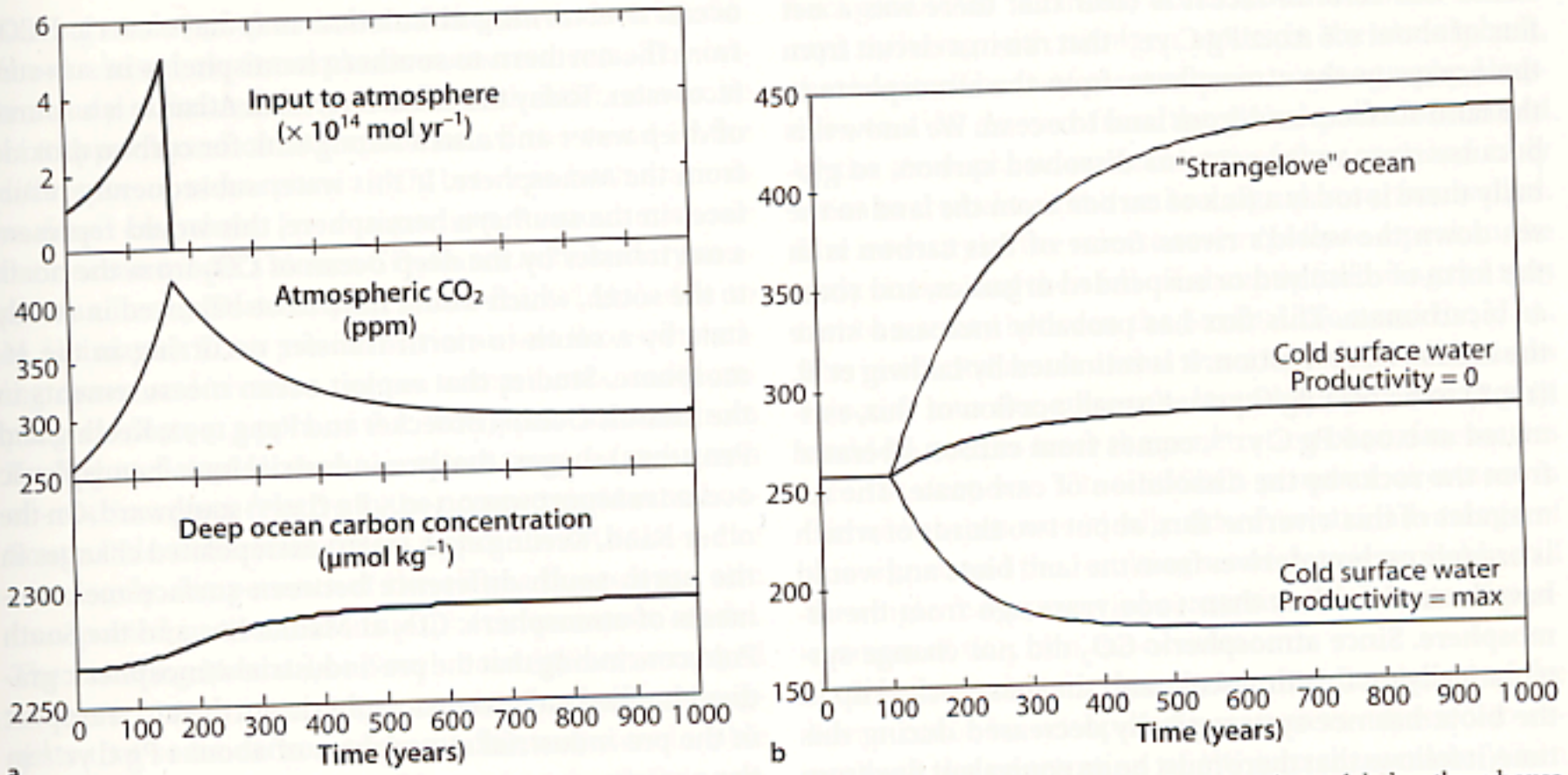

Fig. 5.2. Examples of the behavior of a simple model of the atmosphere-ocean carbon system, in which the ocean is modeled as three boxes (Sarmiento and Toggweiler 1984). **a** Perturbation by an exponentially growing release of CO_2 into the atmosphere that starts at 10^{14} mol yr^{-1} (1.2 Pg C yr^{-1}) and grows at 1% per year for 150 years, then ceases. Atmospheric CO_2 is forced up while the release is growing, but begins to decline by ocean uptake as soon as it ceases. The deep sea is the ultimate repository for most of the released carbon, but concentrations rise only slightly there because the reservoir is so large. **b** Effect of changing the biological pump; 'Strangelove' Ocean (all biological activity ceases), or cold surface ocean productivity ceases, or cold surface ocean productivity raised to the maximum consistent with phosphate concentrations. Changes in biological activity can shift the steady state pre-industrial atmospheric CO_2 concentration by a substantial amount

the effect of the industrial revolution on the carbon cycle. In the model scenario, a release is imposed that grows at 1% per year for 150 years, at which point it abruptly ceases. Atmospheric CO_2 is initially forced up rapidly by the release because the ocean cannot take up CO_2 from the atmosphere as rapidly as it is being added but, as soon as the release is stopped, the concentrations start to decline by uptake to the ocean. After a few hundred years equilibrium is re-established at concentrations only about 30 ppm above the pre-industrial level. The majority of the carbon released ends in the deep sea, but concentrations here increase by only ~1% because this reservoir is so big. Steady state atmospheric concentrations are ~10% higher than previously, and this is because a 1% increase in total carbon in the ocean has a proportionately larger effect on the steady state pCO_2 at the ocean surface. This effect is quantified by the Revelle Buffer factor (β), defined as the fractional change in pCO_2 for a unit fractional change in total carbon content. For average seawater $\beta \sim 10$ (at constant temperature and alkalinity), meaning that a 1% change in total carbon leads to ~10% change in pCO_2 at equilibrium.

In Fig. 5.2b, the effect of changing the efficiency of the 'biological pump' in the oceans is investigated. Increasing net productivity in the 'cold surface water' box of the model (notionally corresponding to the Southern Ocean) removes some carbon from this surface box and rains it down into the deep ocean. The removal of carbon from the surface decreases the carbon content there by a few percent, but this is sufficient to change the equilibrium CO_2 substantially, again due to the high value of β. Atmospheric CO_2 decreases by up to 80 ppm below the previous steady state. Setting the biological pump to zero everywhere (the 'Strangelove' ocean) causes it to increase by about 180 ppm. In these cases no carbon is added to the system in total, but atmospheric CO_2 is affected by modulating processes at the surface ocean so as to change the distribution between ocean and atmosphere.

5.2.2 The Pre-Industrial Steady State

Records obtained from ice core and ice-firn (Indermuhle et al. 1999) show that, before the industrial revolution, the CO_2 concentration in the atmosphere was in the range 280 ±10 ppm for five thousand years. By contrast, from Fig. 5.1 we can see that the residence time for exchange of atmospheric CO_2 to the surface ocean or terrestrial biosphere (the size of the reservoir divided by the flux out of it) is only ~10 years, while the time to adjust to redistribution of carbon between atmosphere and the deep ocean is a few hundred years (Fig. 5.2). It is apparent therefore that the atmosphere was closely in steady state with regard to the net inputs and outputs to the land and oceans before the industrial era. This does not imply that air-sea flux or the air-land flux were each identically zero, only that the sum of these two

fluxes was zero. In fact it is clear that there was a net flux of about 0.6 ±0.2 Pg C yr^{-1} that ran in a circuit from the oceans to the atmosphere, from the atmosphere to the land surfaces and from land to ocean. We know this because river water contains dissolved carbon, so globally there is today a flux of carbon from the land to the sea down the world's rivers. Some of this carbon is in the form of dissolved or suspended organics, and some as bicarbonate. This flux has probably increased since the industrial revolution. It is estimated by Ludwig et al. (1998) to be 0.72 Pg C yr^{-1}. A small portion of this, estimated at 0.096 Pg C yr^{-1}, comes from carbon liberated from the rocks by the dissolution of carbonate. The remainder of this 'riverine' flux, about two thirds of which is organic carbon, derives from the land biota and would have been fixed less than 1 000 years ago from the atmosphere. Since atmospheric CO_2 did not change systematically on this timescale, and the mass locked up in the biota has not systematically decreased during this time, it follows that there must be an equivalent flux from oceans to atmosphere to keep the system in steady state. Whether this flux mostly returns to the atmosphere in river estuaries and the coastal ocean, or whether it is distributed over the global ocean, is unknown at present. It depends in particular on the lifetime against oxidation of the organic carbon being carried by the rivers. Depending on the distribution of this flux, direct estimates of the global atmosphere-ocean CO_2 flux may need to be increased by up to ~0.6 Pg C yr^{-1} before comparison with estimates of how the flux has changed since pre-industrial times (see Table 5.2).

5.2.3 Pre-Industrial North-South Transports

Another aspect of the pre-industrial steady state that is important for our present understanding is the issue of whether there was a north-south asymmetry in the distributions of sources and sinks of CO_2 before the industrial era. This would have given rise to a slight gradient in the atmosphere at that time. There are two possible reasons for thinking that there would be such an asymmetry. First, because most of the land surfaces are in the northern hemisphere and the land was a net sink, whereas most of the oceans are in the southern hemisphere and the oceans were a net source, we might expect an enhanced sink in the north and corresponding source in the south. How large such an asymmetry would be depends on the residence time of the riverine carbon against air-sea transfer once it reaches the sea. If this is measured in decades or longer, then we might expect the net source it engenders to be evenly spread over the surface of the global ocean, in other words partly in the southern hemisphere.

A second reason for believing that there might be a north-south imbalance in pre-industrial time is that the ocean overturning circulation may have carried CO_2 from the northern to southern hemispheres in sub-surface water. Today the northern North Atlantic is a source of deep water and also a strong sink for carbon dioxide from the atmosphere. If this water subsequently resurfaces in the southern hemisphere, this would represent a net transfer by the deep ocean of CO_2 from the north to the south, which would have to be balanced in steady state by a south-to-north transfer occurring in the atmosphere. Studies that exploit ocean measurements in the Atlantic Ocean (Broecker and Peng 1992; Keeling and Peng 1995) suggest that pre-industrial inter-hemispheric ocean transport was 0.3–0.5 Pg C yr^{-1} southward. On the other hand, Keeling et al. (1989) extrapolated changes in the north-south difference between surface measurements of atmospheric CO_2 at Mauna Loa and the South Pole, concluding that the pre-industrial atmospheric gradient implied an inter-hemispheric northward transport in the pre-industrial atmosphere of about 1 Pg C yr^{-1} in the ocean.

These inferred transports can be compared with direct estimates from ocean carbon cycle models. Three ocean carbon cycle models were used to investigate this pre-industrial carbon transport during the first Ocean Carbon Models Intercomparison Program (OCMIP-1) (Sarmiento et al. 2000). None of these models produced a southward, pre-industrial, transport of more than 0.1 Pg C yr^{-1}. At the other extreme was one model that actually produced a northward transport of 0.1 Pg C yr^{-1}. All three OCMIP-1 models revealed a global-ocean carbon loop, where 0.6 Pg C yr^{-1} is transported from the Bering Strait, across the Arctic Ocean, southwards through the Atlantic, across the Southern Ocean, northwards again through the Indian and Pacific Oceans, and finally back to Bering Strait. This loop is entirely oceanic however, and barely affects the atmospheric gradients. During OCMIP-2, there was an effort to test the robustness of the OCMIP-1 conclusions by performing similar analysis on a more diverse group of 12 models. OCMIP-2 found a much larger range of total southward pre-industrial transport, from 0.0 up to 0.7 Pg C yr^{-1}. However, excluding one outlier, southward cross-equatorial transport was less than 0.35 Pg C yr^{-1}.

Furthermore, a separate simulation with one of the OCMIP-1 models has highlighted that the ocean models are missing a 'riverine' carbon flux, and that this affects the pre-industrial north-south transport. Aumont et al. (2001) showed with the IPSL model that simulated southward carbon transport increased by 0.1 to 0.3 Pg C yr^{-1} when riverine carbon, from (mostly northern hemisphere) rivers was added, assuming subsequent transport of this carbon within the ocean and outgassing over the whole ocean surface. The Aumont et al. transport is thus consistent with the transports derived from ocean measurements. On the other hand, there remains a discrepancy between Aumont et al.'s results and the

Keeling et al. (1989) estimate of the pre-industrial difference based on atmospheric measurements. The latter study estimates the pre-industrial difference to be −0.82 ppm based on extrapolation of the trend in the difference of atmospheric CO_2 between both stations vs. fossil emissions. For comparison, Aumont et al. use their ocean model's air-sea CO_2 fluxes as boundary conditions in a 3-D atmospheric model, ('TM2', due to M. Heimann). Their pre-industrial air-sea fluxes, including ocean and riverine carbon components, could explain at most −0.3 ppm of the −0.82 ppm estimate from Keeling et al. (1989): the river effect caused a reduction of −0.4 ±0.1 ppm, relative to the ocean-only Mauna Loa-South Pole difference of +0.1 ppm. In OCMIP-2, the ocean-only components of the air-sea fluxes were also transported in the TM2 atmospheric transport model. The resulting Mauna Loa-South Pole difference ranged from −0.28 to +0.22 ppm. Summing both effects suggests that some carbon cycle models may now be able to simulate up to a −0.7 ppm Mauna Loa-South Pole pre-industrial difference. This preliminary calculation indicates the need for more ocean carbon models to explicitly include the river loop. Meanwhile, the debate concerning the magnitude of pre-industrial ocean carbon transport remains open.

Two recent data-analysis studies confirm the inter-hemispheric difference in atmospheric CO_2 derived by Keeling et al., while offering more spatial detail. These new studies find similar results. However, they differ substantially in their interpretation of the cause of the difference. To explain the difference, Conway and Tans (1999) invoke a large anthropogenic sink in the northern hemisphere, that has been essentially constant over the last 40 years. Conversely, Taylor and Orr (2000) suggest that the cause must be natural. They invoke the 'rectifier effect' – the name given to the gradient set up by covariance between seasonal changes in atmospheric transport and the seasonal variability of atmospheric CO_2 concentrations (Pearman and Hyson 1986).

5.3 How Big is the Global Ocean Sink?

During JGOFS we have been able to estimate the global ocean sink by several different independent or quasi-independent methods. Broadly, these are based on three different approaches, models, atmospheric observations and ocean observations, which we describe below.

5.3.1 1-D Models Calibrated with ^{14}C

This approach has been used since the 1970s and was first made possible by the GEOSECS measurements made by Östlund and colleagues of the distribution of ^{14}C in the oceans (Östlund et al. 1987). There is a natural background of ^{14}C in the oceans, derived from cosmic rays colliding with nitrogen atoms in the atmosphere, that has itself been of great value in oceanography. However, the ^{14}C derived from the global pollution caused by the atmospheric nuclear tests of the 1950s and early 1960s overwhelmed the natural signal in surface waters. The intensity of the release rose rapidly to a peak in the early sixties, and then fell off abruptly following the 1963 test ban treaty between the Soviet Union and the USA. The incidental result of this was a 'spike' of radiotracers injected into the atmosphere and surface ocean that could be used to trace the penetration of surface waters into the deep sea. The GEOSECS program of cruises in the early 1970s was ideally timed to take advantage of this signal, and the resulting set of data is probably still the single most powerful constraint on the rate of penetration of CO_2 into the oceans.

Simple models for the overturning circulation of the ocean could be set up and parameters adjusted to reproduce the penetration of ^{14}C into the oceans. When these models were first used to calculate the uptake of fossil fuel CO_2 in response to increasing atmospheric concentrations, answers of the order of 2 Pg C yr^{-1} were obtained. These were compatible with the paradigm of the time, that the land biosphere was neutral with respect to the uptake and release of carbon, so that the difference between the rate of release by fossil fuel burning and the rate of accumulation in the atmosphere was all due to ocean uptake. Since that time, ideas about the sink or source nature of the land biosphere have changed substantially, but the estimate of the ocean sink has remained quite stable.

The success of even simple models in constraining ocean uptake is due to the parallel between the uptake of fossil fuel CO_2 and that of bomb radiocarbon, but this parallel is not exact. For example, the rise in atmospheric CO_2 has taken place over a period of considerably more than a century whereas the bomb signal was over in less than a decade. Furthermore, the time constant for exchange with the atmosphere of injected ^{14}C is an order of magnitude longer than that of ^{12}C (Broecker et al. 1985). The reliability of the models will decrease over longer time scales, although performance over longer times can be constrained by requiring that natural ^{14}C as well as bomb-^{14}C concentrations are reproduced by the models (Siegenthaler and Joos 1992).

5.3.2 3-D Models of the Ocean Carbon Cycle

In the late eighties global circulation models were first combined with simple carbon models of the ocean to produce ocean carbon models capable of diagnosing the fossil fuel sink (Sarmiento et al. 1988). This approach has been refined and developed over the past decade, and there are now many such models in existence. A

major initiative under international JGOFS has been the evaluation of the many different such models in the Ocean Carbon Models Intercomparison Programs, OCMIP-1 and 2. These models are one of the best means to test current ideas of the ocean carbon cycle, and as such we repeatedly refer to them in this chapter. Of their many uses, perhaps the most important has been to improve our estimates of the ocean sink for anthropogenic CO_2.

Compared to the earlier generation of models, these have three-dimensional circulations derived from finite-difference solutions of the equations for conservation of mass and momentum. The boundary conditions used to initiate the equations that govern the circulation are typically surface ocean wind stress, and fluxes of heat and fresh water. The resolution is typically two to four degrees in the horizontal and 12 to 30 levels in the vertical, and the forcing is usually climatological and resolved to monthly or finer time scales. These models reproduce the main features of the ocean circulation including the major wind-driven currents and zones of surface convergence and divergence. Early estimates of the anthropogenic uptake during the 1980s made with these models were consistent with the results of simpler models, for example 2.0 ±0.6 Pg C yr^{-1} (Siegenthaler and Sarmiento 1993), and 2.0 ±0.5 Pg C yr^{-1} (Orr 1993). Such estimates were the main basis of the widely-quoted IPCC value for the ocean sink of 2.0 ±0.8 Pg C yr^{-1} (Houghton et al. 1990, 1995).

To help evaluate model uncertainties, and to set the stage for improving predictability, we show here results from OCMIP-2 of simulations of anthropogenic CO_2 in thirteen climatologically forced, coarse-resolution ocean models (Table 5.1). The simulated global uptake for the 1980s was in the range 1.65 to 2.51 Pg C yr^{-1}, with a mean of 1.99 Pg C yr^{-1}. This range falls within the spread of flux estimates from previous compilations of 1-, 2-, and 3-D ocean model results as given above. The wider uncertainties of the earlier studies reflect mainly the additional uncertainties due to our imperfect understanding of the global distribution of bomb ^{14}C, which is used to calibrate ocean models. Additionally, the OCMIP-2 range is similar to that found with four models during OCMIP-1, i.e., 1.6 to 2.1 Pg C yr^{-1} (Orr et al. 2001).

Table 5.1. Change in global annual air-to-sea flux of CO_2 (Pg C yr^{-1}) from pre-industrial value (1765)

Model	1980–1989	1990–1999
PRINCE	1.65	1.98
IPSL.DM1 (HOR)	1.67	1.98
LLNL	1.78	2.08
CSIRO	1.78	2.11
MIT	1.91	2.29
NCAR	1.93	2.30
PRINC2	1.93	2.32
IPSL (GM)	1.97	2.36
MPIM	2.01	2.43
SOC	2.01	2.39
IPSL.DM1 (GM)	2.03	2.43
IGCR	2.05	2.47
PIUB	2.11	2.52
AWI	2.14	2.58
NERSC	2.38	2.84
UL	2.51	3.04
Mean of models	1.99	2.38

Acronyms are: *AWI* (Alfred Wegener Institute for Polar and Marine Research), Bremerhaven, Germany; *CSIRO*, Hobart, Australia; *IGCR*/CCSR, Tokyo, Japan; *IPSL* (Institute Pierre Simon Laplace), Paris, France; *LLNL* (Lawrence Livermore National Laboratories), Livermore, California, USA; *MIT*, Boston, MA, USA; *MPIM* (Max Planck Institut für Meteorologie), Hamburg, Germany; *NCAR* (National Center for Atmospheric Research), Boulder, Colorado, USA; *NERSC* (Nansen Environmental and Remote Sensing Center), Bergen, Norway; *PIUB* (Physics Institute, University of Bern), Switzerland; *PRINCE*ton (Princeton University [AOS, OTL]/GFDL), Princeton, NJ, USA; *SOC*

5.3.3 ^{13}C Changes with Time in the Ocean

The $^{13}C/^{12}C$ ratio of carbon dissolved in the ocean is changing as fossil fuel carbon invades the surface – termed the ^{13}C Suess effect. Surveys of $\delta^{13}C$ spaced many years apart can therefore be used to calculate the invasion rate independently of other methods. Quay et al. (1992) and Sonnerup et al. (1999) report on this technique, with the most recent estimate giving 1.9 ±0.9 Pg C yr^{-1} as the rate of carbon uptake over the period 1970–1990. This method is potentially valuable as an independent validation of other methods, but the error bars quoted are comparatively large. In addition, there are some problems with possible offsets in some of the early ^{13}C data sets, as reported by Lerperger et al. (2000), who present a set of Pacific data suggesting substantially lower values for ocean uptake.

5.3.4 Atmospheric Observations

Below the stratosphere, the global atmosphere has a time constant for mixing on the order of one year, much faster than that of the ocean, where even the surface requires decades to homogenise. Observations at a few representative sites in the atmosphere can therefore be extrapolated to the entire globe with an accuracy that would require orders of magnitude more effort if it were to be achieved from marine observations alone. As a result, comparatively sparse atmospheric observations impose powerful constraints on the global ocean up-

High precision observations of atmospheric oxygen (actually the ratio of O_2/N_2) of the kind initiated by R. F. Keeling (Keeling and Shertz 1992) can be combined with atmospheric CO_2 observations to give a direct estimate of the marine and terrestrial sinks of anthropogenic CO_2. In Keeling's method, the rate of decline of atmospheric oxygen and increase in CO_2 in the atmosphere are estimated from atmospheric time series. Burning of fossil fuel releases CO_2 and consumes oxygen in a known molar ratio of about $O_2:CO_2 \approx 1.4$, while net biological uptake or release of carbon and oxygen by the land vegetation occurs in a ratio $O_2:CO_2 \approx 1.1$. Uptake of fossil fuel carbon by the ocean is not accompanied by any net exchange of oxygen, i.e., $O_2:CO_2 \approx 0$, and it is assumed that the ocean is neither a source nor sink of oxygen when averaged over a year. Two equations, one for the CO_2 and one for the O_2 change, can then be written and solved for the size of the land and ocean sinks. This method has since been applied to more extensive data sets (Battle et al. 2000).

Atmospheric oxygen is only one example of measurements in the atmosphere that can be used to help separate the oceanic and terrestrial components of the sink for anthropogenic CO_2. Another is the interpretation of atmospheric ^{13}C variations. Fractionation of ^{13}C relative to ^{12}C during photosynthesis is substantial, while ocean-atmosphere exchange results in little fractionation. Thus seasonal and inter-annual changes in the $\delta^{13}C$ of the atmosphere can similarly be related to the strength of these sinks. Using data from a network of atmospheric sampling stations in an atmospheric transport model, information can be obtained about the distribution around the world of the sources and sinks. Addition of measurements besides CO_2 and O_2 that discriminate between ocean and land surface also improves the estimate. This 'inversion' technique can potentially synthesise many different measurements that provide constraints on the sources and sinks to give an objective best estimate of the ocean sink. Bousquet et al. (2000), Rayner et al. (1999) and Langenfelds et al. (1999) are recent examples of estimates made by the atmospheric inversion technique.

As always, caution is needed in the application of these methods. An accurate assessment of the uncertainties in the data has to be incorporated into the analysis. If noisy or biased data are used without allowance being made, the resulting estimates of sinks are similarly noisy and biased. Similarly, the assumptions going into the model will bias the outcome if they are incorrect. For example, Keeling's method is sensitive to the assumption that oxygen in the ocean is in steady state, which is questionable if the oceans have begun to warm or change their degree of stratification, (as further discussed below). It also assumes specific values for $O_2:CO_2$ ratios during fossil fuel burning and vegetation uptake, which are not invariant or precisely known.

5.3.5 Observations of the Air-Sea Flux

Conceptually, the simplest way to specify the global flux of CO_2 from the atmosphere into the oceans is to measure it (over all the oceans, and all the time). Unfortunately, until very recently (see section on 'Gas Transfer Velocity') the direct measurement of CO_2 flux has been too insensitive to give useful results even at one place and one time. The approach followed over the past several decades has therefore been to split the problem into two parts, for one of which at least we do have an accurate means of measurement. Subtracting the two equations (5.1) to obtain the net flux, we have:

$$F_{net} = F_{air\text{-}sea} - F_{sea\text{-}air} = K\Delta pCO_2$$

where ΔpCO_2 is the difference between the atmospheric and surface ocean partial pressures of CO_2. The gas transfer coefficient K is normally further divided into the product $k_v\alpha$, where k_v is the gas transfer velocity (or piston velocity) and α is the solubility of carbon dioxide, which is accurately known as a function of temperature and salinity (Weiss 1974).

$$F_{net} = k_v\alpha\Delta pCO_2$$

This equation expresses the air-sea flux as a product of a readily measurable chemical gradient across the sea surface ($\alpha\Delta pCO_2$), and a variable gas transfer velocity k_v that expresses the ease with which a molecule of gas can pass from the gaseous to the dissolved phase or vice versa. The gas transfer velocity is not so easily measured, but progress has been made in parameterising it. We discuss the transfer velocity below.

Measurements of surface pCO_2 or ΔpCO_2 have been made since the early 1970s from research vessels, and more recently from commercial ships of opportunity and moored or drifting buoys. JGOFS activities have contributed to this database enormously, and in truly international fashion, during the nineties. Major contributions came both from the global CO_2 survey sponsored by JGOFS and WOCE, and from the many process and monitoring studies occurring in different parts of the world at a national and international level.

Syntheses of these data have been published (Takahashi et al. 1997, 1999; Lefèvre et al. 1999) and the synthesis program is ongoing. Globally the database now exceeds one million measurements. The syntheses to date have been in the form of monthly or seasonal climatologies, in which it is assumed that the major variability in pCO_2 at a given site is on a seasonal cycle, so that data from different years but the same time of year can be pooled to give a meaningful average. A major uncertainty in such analyses is how to deal with the continuous increase in atmospheric CO_2 that has occurred during the period of the meas-

urements. Though the majority of the data are from the 1990s, data have been collected over a period spanning thirty years. During this time atmospheric pCO_2 has increased by around 40 ppm, about five times larger than the mean difference between atmosphere and ocean, so this is not a small correction. In regions where the surface waters have a long residence time (years to decades) we can expect sea-surface pCO_2 to tend to increase towards the atmosphere, whereas in regions where the surface is being rapidly replaced by deeper water this tendency would be less. Takahashi et al. therefore assume that for all waters equatorward of 50° N and 50° S, surface ocean pCO_2 has increased at the same rate as in the atmosphere. This corresponds to the subtropical gyres where we expect water to remain for a long time at the surface. Poleward of these latitudes they assume either no increase in pCO_{2sea} or an increase at half the rate of the atmosphere. These assumptions are of necessity arbitrary and introduce uncertainties into derived fluxes.

The global distribution of the air-sea flux of CO_2 over the world ocean derived by Takahashi et al. (2000) is shown in Fig. 5.3. By integrating over the ocean surface of Fig. 5.3, we can arrive at an estimate of the size of the global air-to-sea flux. Takahashi et al. quote 2.17 Pg C yr^{-1} for this flux, corrected to 1995. This is an estimate of the actual air-sea flux at that time. To allow for direct comparison with estimates by other methods (see Table 5.2) a 'riverine' component of up to 0.6 Pg C yr^{-1} should probably be added to this, corresponding to the steady-state sea-to-air flux in pre-industrial time. However, it is not at present known how much of the riverine flux arises from the open ocean, and how much from wetlands, estuaries and the near-shore ocean.

The error bars on this observational estimate are large. Major sources of uncertainty are the interpolation to account for the rise in atmospheric CO_2 described above, the uncertainty on parameterization of the gas transfer velocity (described more fully below) and the fact that there remain some areas of the world ocean very sparsely covered, particularly the South Pacific and Southern Ocean. (The substantial difference between Takahashi et al.'s 1997 and 1999 estimates derives in part from the inclusion of a data set, due to A. Poisson and colleagues, covering the Southern Indian Ocean.) Because of these uncertainties, the integration to obtain the global net flux is presently not a particularly useful constraint on the global ocean sink. The value of the global pCO_2 survey is immense however, for it gives us a detailed picture of the relative importance of source and sink regions and how these vary seasonally. In the large areas where the data coverage is good, this description is an important test for any model (either conceptual or numerical) of the processes governing air-sea flux of carbon. The global pCO_2 survey shows how the ocean 'breathes', and as it is further refined this information grows ever more valuable.

5.3.6 Preformed Total Carbon Methods and the Ocean Inventory of CO_2

The global survey of CO_2 sponsored by WOCE and JGOFS, consisted of full-depth sections of inorganic CO_2 over all the major oceans. These measurements were made to an accuracy of order 1 μmol kg^{-1} (0.05%) in total carbon, with intercalibration maintained across the many groups and long time interval by the production of thousands of standards to this high accuracy (A. G. Dickson, ms in preparation). This effort has given us a three-dimensional picture of the distribution of inorganic carbon in the ocean of unprecendented detail and accuracy. It will likely serve as the basis of the description of the CO_2 distribution in the oceans for decades to come.

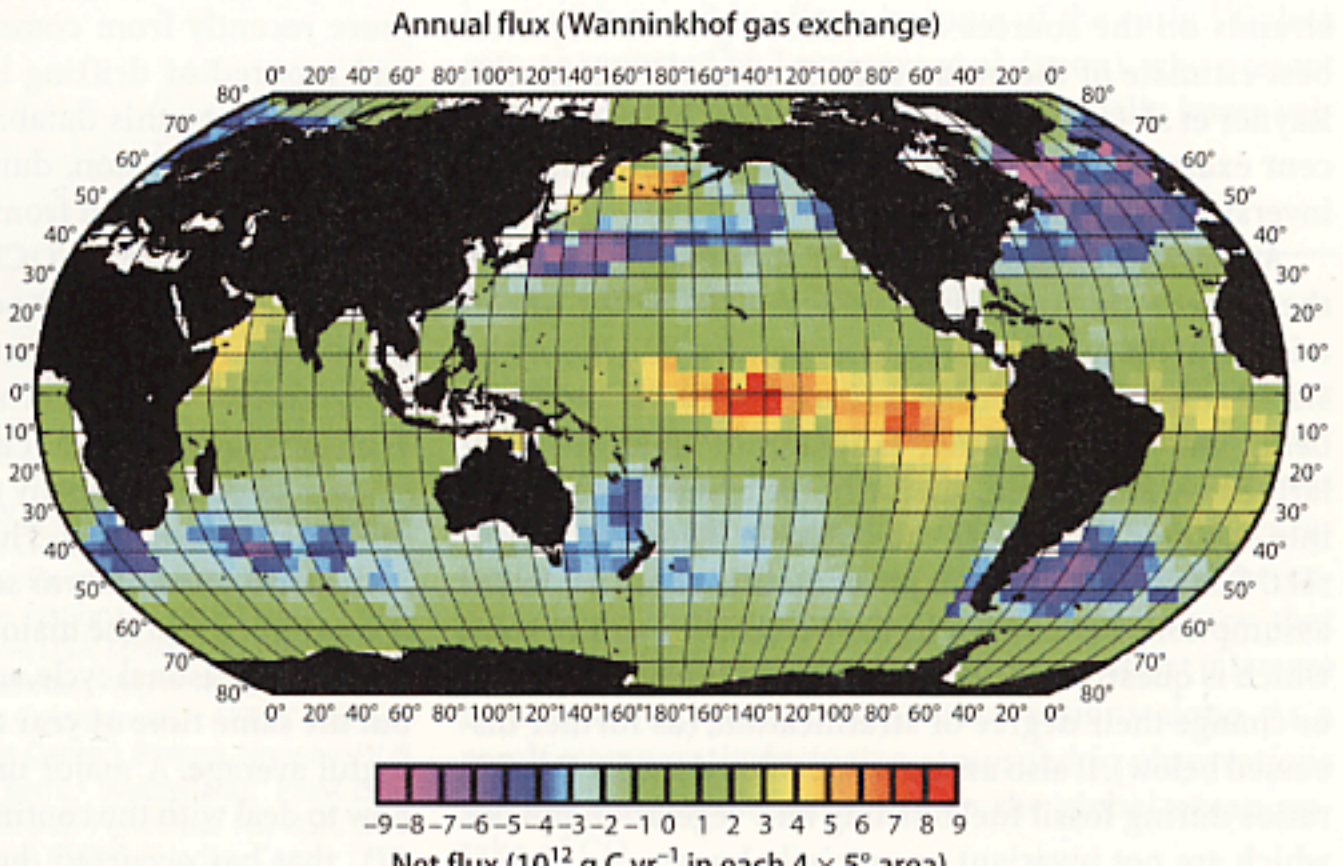

Fig. 5.3.
The global, annual distribution of air-sea flux of CO_2 derived from pCO_2 measurements in the surface ocean (reprinted from Takahashi et al. (2002)). These estimates are based on the air-sea gas exchange equation, with ocean pCO_2 data collected over several decades, but corrected to 1995 under assumptions described in the text. The Wanninkhof (1992) gas exchange-wind speed relationship was used

In using this resource to calculate the amount of anthropogenic CO_2 taken up by the oceans, the difficulty is to separate the man-made signal from the natural processes, which are larger and normally dominate the variations in carbon content. A method for making this separation was introduced in the 1970s (Brewer 1978; Chen and Millero 1979) and an improved technique due to Gruber et al. (1996) has now been applied by several authors to parts of the global data base (Gruber 1998; Feely et al. 1999; Sabine et al. 1999).

In detail the method now being used is fairly complex, but in outline what is done is to estimate what the total carbon content of a given sample would have been pre-industrially and to subtract this from the presently observed value to give the excess carbon. To do this, Gruber et al. make use of a quasi-conservative tracer that is invariant with respect to biological processes. Soft-tissue remineralisation is accounted for by tracking the oxygen content and carbonate remineralisation is accounted for by corrections to alkalinity. The tracer is defined by:

$$\Delta C^* = C_m - R_{C:O}[(O_2)_{eq} - (O_2)_m] - 0.5\{TA_m - TA_0 - R_{N:O}[(O_2)_{eq} - (O_2)_m]\} - C_{eq}$$

where C is total inorganic carbon, and O_2 dissolved oxygen. The subscript 'm' signifies measured quantities, while 'eq' refers to equilibrium with the pre-industrial atmosphere, $R_{C:O}$ and $R_{N:O}$ are Redfield ratios of carbon and nitrate to oxygen utilization (both negative in sign), TA is the total alkalinity and TA_0 the preformed total alkalinity, determined as a function of temperature, salinity and nutrient content.

If remineralization of organic and carbonate carbon were the only in situ processes that could cause carbon content to change once water leaves the surface layer, this tracer for change in 'preformed total carbon' would be approximately conservative. Anthropogenic carbon content is calculated as the difference between the preformed total carbon calculated for a given sample, and that estimated for the sample pre-industrially. The method of calculating this pre-industrial value varies. Mixing is assumed to occur only along density surfaces (isopycnals). If an end member can be found on such a surface at sufficient distance from the surface, the anthropogenic influence there can be assumed to be negligible, and this allows an estimate of the pre-industrial preformed total carbon. In other situations, transient tracers such as the CFCs or tritium-helium can be used to estimate a 'ventilation age' for the sample. This can be related to the degree to which surface pCO_2 would have been increased at the time the water mass was ventilated.

The information retrieved by the inventory technique is invaluable for global carbon studies because it relates specifically to the total uptake of the ocean since the industrial revolution, a variable that is difficult to ascertain by any other observational method. The uncertainty in the sink for individual ocean regions has been estimated as ~20% (Gruber 1998). The total amount of carbon burned as fossil fuel, and the amount by which atmospheric CO_2 has increased, are well known (to better than 10%), so the net uptake or release of the land biosphere can be calculated by difference from these figures with reasonable accuracy. The approximations involved in back-calculating pre-industrial pre-formed carbon for water masses are the chief uncertainty of the method.

Table 5.2 Recent estimates of the ocean sink for CO_2

Reference	Method	Mean (Pg C yr^{-1})	Uncertainty (Pg C yr^{-1})	Period covered
	Model estimates			
Thirteen OCMIP-2 models	Ocean carbon cycle models	2.0	0.3 (2–σ between models)	1980–1989
Thirteen OCMIP-2 models	Ocean carbon cycle models	2.4	0.5 (2–σ between models)	1990–1999
Takahashi et al. (1999)	Surface ocean pCO_2	1.5[a]	0.7	Corrected to 1990
Takahashi et al. (1999)	Surface ocean pCO_2	2.2[a]	1.1	Corrected to 1995
Sonnerup et al. (1999)	Oceanic ^{13}C change	1.9	0.9	1970–1990
	Atmospheric inversions			
Battle et al. (2000)	O_2/N_2 and CO_2, ^{13}C used as check	2.0	0.6 (1–σ variability)	1991–1997
Keeling et al. (1996)	O_2/N_2 and CO_2	1.9		1991–1994
IPCC (Hougton et al. 2001)	O_2/N_2 and CO_2	1.7	0.5 (1–σ variability)	1991–2000
Ciais et al. (2000)	$^{12}CO_2$ distributions	1.5	0.5 (1–σ variability)	1985–1995
Kaminski et al. (1999)	$^{12}CO_2$ distributions	1.5	0.4 (1–σ variability)	1980–1989
Kheshgi et al. (1999)	Carbon cycle model (^{12}C, ^{13}C, ^{14}C)	1.7	0.7 (90% confidence int.)	1980–1989
Kheshgi et al. (1999)	O_2/N_2, ^{12}C, ^{13}C	2.1	0.3 (1–σ variability)	1980–1996

[a] These figures refer to the actual, observed flux across the air-sea interface, whereas all the other figures in the table refer to the change from the pre-industrial steady state. As such, for comparison with the other figures an (unknown) proportion of the riverine flux of

5.3.7 Summary of Recent Estimates of the Ocean Sink

In Table 5.2 we have drawn together recent estimates of the ocean sink for the periods of the 1980s and 1990s. Overall, at the present time there is little reason to update the 'canonical' estimate of 2.0 Pg C yr^{-1}. However, it is notable that, taking all the methods into account, we are still unable to be confident in the size of the sink to much greater than about 30%. In particular, the models consistently predict that the sink should have increased by about 20% between these two decades, as the atmospheric concentration continues to rise, and that this trend might be expected to continue in the coming decades. The O_2/N_2 method meanwhile, especially as quoted in the recent IPCC third assessment report, gives a clearly lower value for the decade of the 1990s than do the model estimates. At the time of writing, the cause of this discrepancy is unknown. One possibility is that it is due to a breakdown in the assumption that the ocean is a zero net source of oxygen. Studies have suggested there should be inter-annual variation in the net source of oxygen from regions subject to seasonal convection such as the North Atlantic (McKinley et al. 2000) and it may be that convection is becoming globally less vigorous and deep as a result of surface warming and increased fresh water runoff. If so, this would be one of the first indications of that global change is beginning to affect the overturning properties of the ocean.

5.4 What Processes Control Air-Sea CO_2 Flux?

The ocean sink, integrated over the whole ocean and periods of a decade, is controlled mainly by the rate of vertical mixing and overturning of the ocean – how quickly surface waters penetrate into the interior. On shorter time and space scales a more complex pattern has emerged from the global survey. In detail we cannot as yet perfectly explain this pattern, but in broad outline, it is readily understood as an interplay between thermodynamic, biological and hydrodynamic forcing of surface pCO_2. (The terms 'solubility pump', and 'biological pump' are frequently used to refer to the thermodynamic and biological forcings, but the important role of circulation and mixing is not obvious using this terminology). The biological effect is due to the local influence of biological activity as it varies from place to place and seasonally. The hydrodynamic effect is the influence of circulation and convection in changing surface water carbon content by mixing it with higher concentrations from greater depth. The thermodynamic effect is the influence of temperature on the solubility of CO_2 and its distribution between carbonate, bicarbonate and dissolved gas. This last is the easiest to quantify: other factors being constant, heating seawater causes pCO_2 to increase by an accurately known amount, about 4% per °C, and cooling does the reverse (Takahashi et al. 1993). Surface water that is warming will therefore tend to have high pCO_2 and be a source to the atmosphere, while cooling water will be a sink. Since the time for equilibration of the CO_2 system with the atmosphere is long (~1 year) compared to the time for thermal equilibration of the mixed layer (a few months), this thermal CO_2 signal may remain measurable even after the thermal forcing has ceased.

5.4.1 Patterns in the Global Survey

The most notable feature on the air-sea flux map (Fig. 5.1) is the equatorial Pacific CO_2 'bulge'. In non-El-Niño years, the Eastern equatorial Pacific is a strong and continuous source of CO_2 to the atmosphere – the strongest oceanic source on Earth. This is due to the upwelling of water into the surface, forced by the equatorial divergence. Subsurface waters have a relatively higher carbon content than the surface as a result of the downward fractionation due to the biological and solubility pumps. More importantly, as the water enters the surface layer it is heated strongly, causing it to begin degassing CO_2 to the atmosphere. The biological effect tends to offset this flux by fixing nutrients and CO_2 out of the newly upwelled water. However, biological CO_2 drawdown in the equatorial Pacific is strongly iron-limited, as shown during JGOFS by bottle incubations (Fitzwater et al. 1996) and in situ fertilizations (Cooper et al. 1996). The biological pump is therefore comparatively inefficient in this region (Murray et al. 1994), and this increases the net CO_2 efflux. All regions of upwelling in the tropics or subtropics may be similarly expected to be sources of atmospheric CO_2, for example the Arabian Sea during the Southwest Monsoon (Sabine et al. 2000), or the Coast of Peru and Chile (Torres et al. 1999). In coastal upwelling systems, net biological drawdown is greater than in the equatorial Pacific, presumably because of a greater supply of available iron.

Warm, poleward-travelling water currents lose heat to the atmosphere and therefore tend to be sinks for atmospheric CO_2. The regions where cooling is strongest are the western boundary currents, particularly the Gulf Stream and the Kuroshio in the Pacific. In the North Atlantic, there is an overall northward drift and cooling of the water as a result of the Atlantic meridional overturning circulation (MOC) and this contributes to a net undersaturation in CO_2 throughout the region north of the subtropical gyre. Furthermore, net biological export is also high. The biological pump in the North Atlantic is efficient, removing most of the nitrate and phosphate in the surface waters, as a result of the ready supply of

iron in the form of atmospheric dust from the surrounding land, particularly the Sahara desert. Both the thermodynamic and the biological effects therefore tend to make the region a net sink for atmospheric CO_2, and the North Atlantic and Nordic Seas are the strongest consistent sink regions in the world ocean.

Other things being equal, strong net sink regions of the ocean should tend to be coincident with regions where water that is cooling or has recently been cooled is at the surface. Because this implies increasing density, such regions are likely to be formation zones for subsurface water. By contrast, the strongest net source regions are warm-water upwelling zones. Again, other things being equal, regions where the biological utilization of nutrients is efficient should be stronger sinks, while 'High nutrient low chlorophyll' (HNLC) regions, where biological utilization of CO_2 is inefficient, should be stronger sources. This reasoning is qualitatively consistent with the major features of the pCO_2 survey. Thus for example, the sink region in the Southern Indian Ocean and in the South Atlantic in the Brazil-Malvinas regions (Fig. 5.3) are located in the formation zones for Antarctic Intermediate Water, which is the major source of thermocline waters for the world ocean. Biological activity is also particularly strong in the Southwest Atlantic, due perhaps to relatively abundant iron supply from the nearby Patagonian Shelf or from windblown dust. The Southern Ocean south of the Polar front is a site of strong upwelling, and also an HNLC zone, so might be expected to be a source zone by this reasoning, though much less marked than in warm-water upwellings because in these cold waters the contribution of heating to raising surface pCO_2 will be absent. In fact, in winter at least, the upwelling water is probably being cooled rather than heated. Measurements south of the Polar front (of which there are very few) suggest the region today is approximately neutral with respect to the atmosphere.

5.4.2 Comparison Using Models

Ocean carbon models enable us to compare quantitatively our expectations with the data. Here, we compare the outputs of models both with the data and with each other. Furthermore, in the models we can decompose the fluxes into the pre-industrial steady-state and anthropogenic components, and the pre-industrial component into solubility-driven and biologically driven parts – impossible to do with the observations, which represent the sum of all the processes occurring simultaneously. Anthropogenic uptake was determined in the OCMIP models as the difference between the model uptake in 1765 and that in 1995. To separate the biological and solubility effects, the models were run for two equilibrium simulations:

a Abiotic – the solubility component which includes carbon chemistry and realistic gas exchange between surface ocean and atmospheric CO_2 (held to 278 ppm for the preindustrial case);
b Biotic – the solubility plus biological components, together.

A measure of the steady-state biological fluxes can be found from the difference between the two simulations.

Sea-to-air fluxes decomposed into these components are displayed as zonal integrals for the global ocean in Fig. 5.4. All the solubility simulations exhibit ocean outgassing in the tropics and uptake in the high latitudes, as expected if high-latitude waters are cooling and sinking while the tropical upwellings are warming. Additionally, the biological component counteracts the solubility component either by bringing respired CO_2 (produced by bacterial degradation of organic matter) to the surface via upwelling and deep convection (mostly in the high latitudes), or by consuming CO_2 at the surface via photosynthesis (mostly in the subtropical gyres and the tropics). Anthropogenic fluxes are generally smaller than natural fluxes, but the contribution from the modern anthropogenic component is not negligible.

Figure 5.5 compares the distribution of the total (anthropogenic plus pre-industrial) fluxes predicted by the models with the climatology of Takahashi et al. (Fig. 5.3, redrawn as the first two panels of Fig. 5.5). The zonal integrals of these distributions are given in Fig. 5.6. All the models predict the equatorial CO_2 bulge, and the strong sinks in the North Atlantic and associated with the Kuroshio in the Northwest Pacific, as also seen in the data. The models show greatest agreement with each other and with the data in lower latitudes (40° S to 40° N).

But in detail the model distributions differ quite substantially, the disagreement being greatest in the Southern Ocean. It is important also to remember that the climatological fluxes represented by the data may be in error for the reasons described above. In particular, Takahashi et al. assumed that at high latitudes, the ocean pCO_2 has not increased, or has increased at only half the rate of the atmosphere, over recent decades. At low latitudes they assumed it has tracked the atmosphere. The models suggest that the low-latitude assumption is probably reasonable, but that at high latitudes the ocean pCO_2 does increase. Hopefully, it will soon be possible to use the models to examine the uncertainties introduced by the assumptions used in constructing the data-based climatologies.

The distribution of the anthropogenic carbon dioxide fluxes in isolation from the natural signals are examined in Fig. 5.7a, while Fig. 5.7b shows the storage of anthropogenic CO_2. As discussed above the models agree well on global mean anthropogenic uptake. General patterns of regional uptake are also grossly similar between

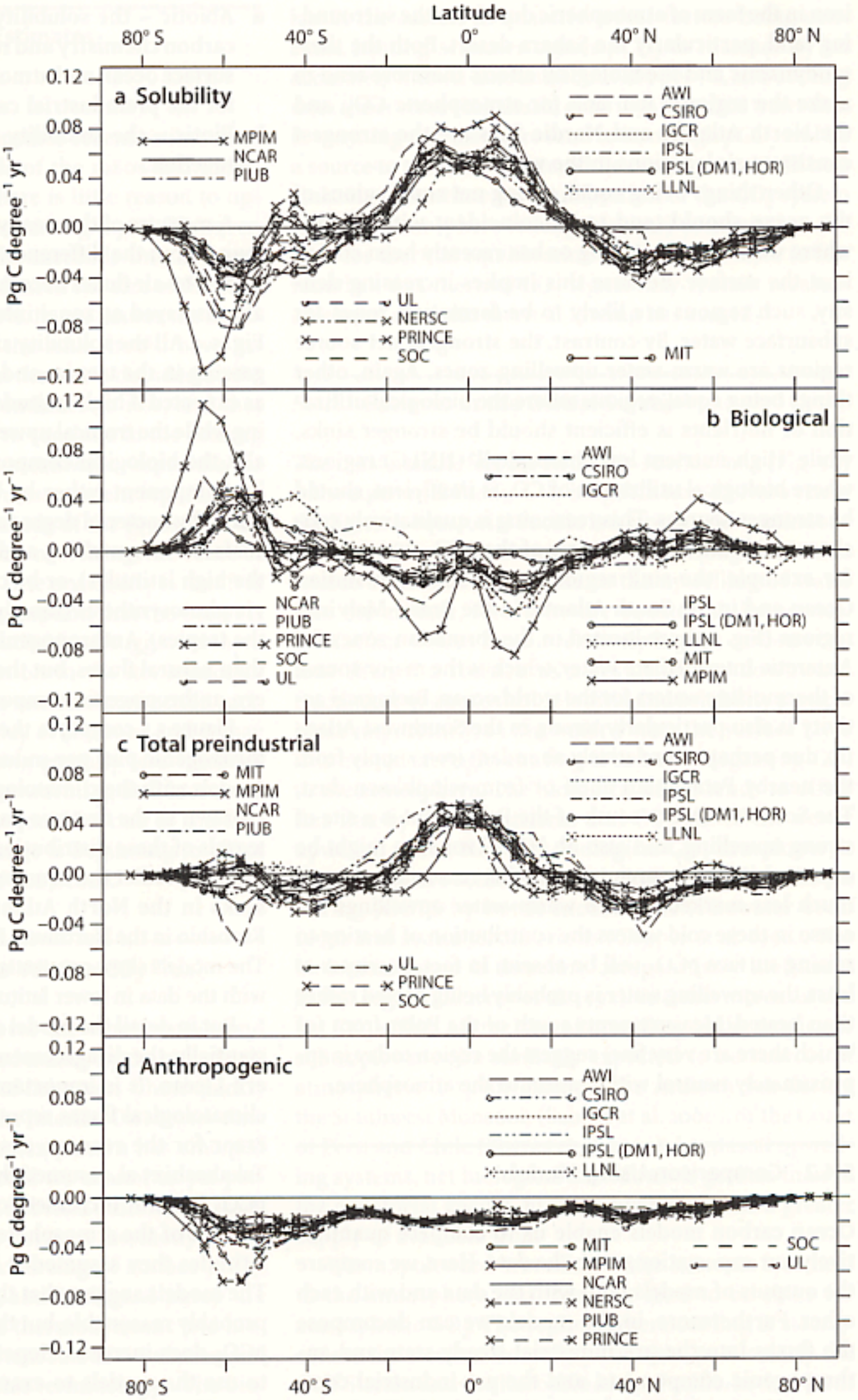

Fig. 5.4.
The zonally integrated sea-to-air flux of CO_2 for the global ocean as predicted by the OCMIP models. The flux is separated into **a** the solubility component, with realistic gas exchange, **b** the biological component only, **c** the sum of $a + b$, i.e., the total natural flux, and **d** the component due to anthropogenic change during 1765 to 1995. The biological component **b** is determined by difference between the 'biotic' and 'abiotic' simulations, described in the text

the OCMIP-2 models, with uptake highest in the high latitudes and at the equator, i.e., in zones where deep waters uncontaminated with anthropogenic CO_2 communicate readily with the surface via upwelling and convection. Low fluxes are evident in the subtropics, where surface waters have had longer to equilibrate with the atmosphere. However, the models disagree substantially about local patterns of anthropogenic carbon uptake. Large differences in model uptake are found in the Southern Ocean, in the tropics, and in the North Atlantic. When ocean surface area is taken into account, the largest differences between models are found south of 30° S, which occupies about one third of the surface of the entire ocean.

As opposed to the large difference in uptake of anthropogenic CO_2, there is surprising agreement among

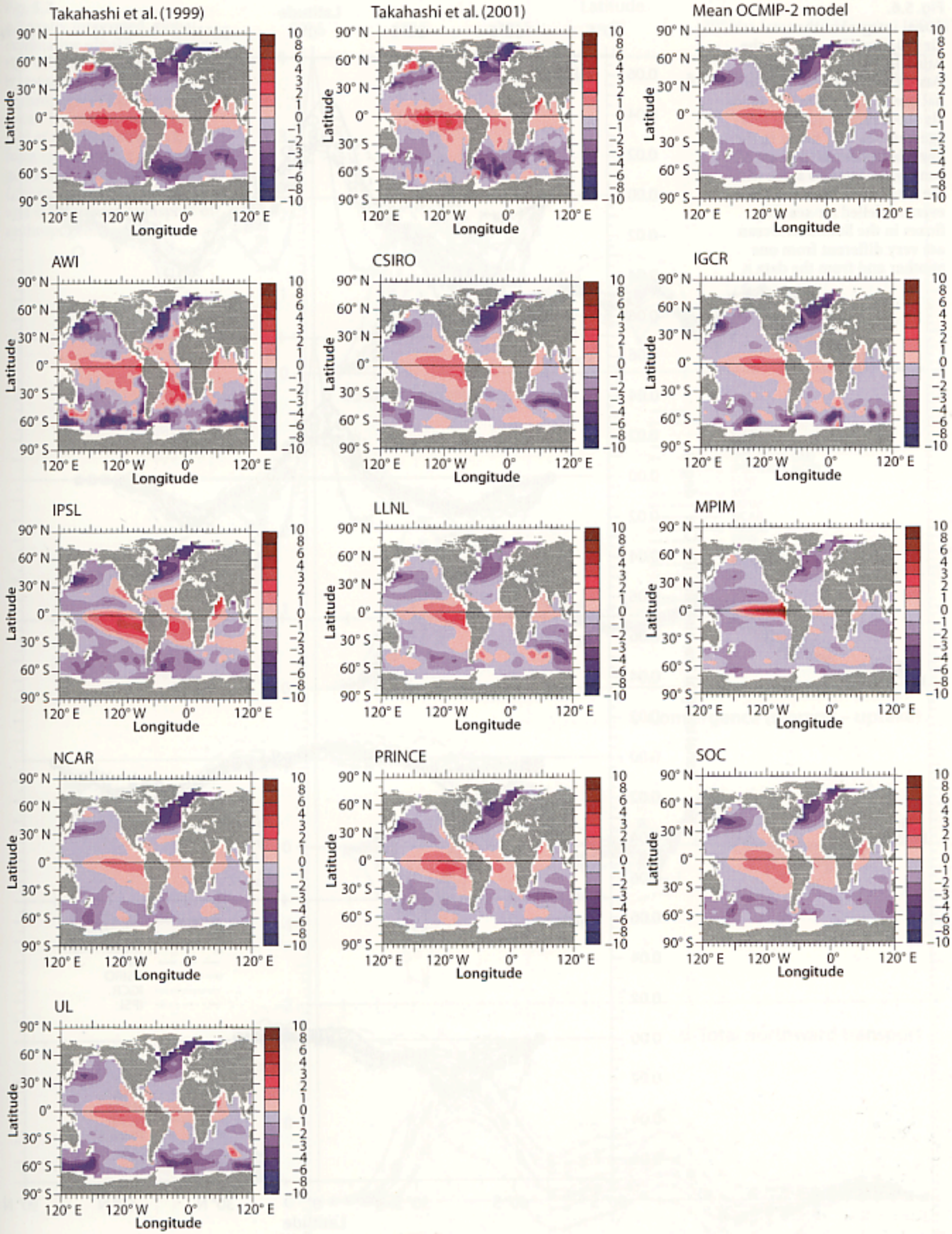

Fig. 5.5. Model and data-based estimates of the annual mean, sea-to-air CO_2 flux in 1995. Observed fluxes are based on pCO_2 observations that were interpolated in space and time to a climatological grid (Takahashi et al. 1999; Takahashi et al. 2002). For consistency, these gridded ΔpCO_2 data fields were then multiplied by the same gas exchange fields used for the OCMIP-2 simulations. The monthly OCMIP-2 gas exchange field is based on satellite observed winds and the gas exchange formulation of Wanninkhof (1992) (see *http://www.ipsl.jussieu.fr/OCMIP*). The model flux fields represent the total sea-air flux, obtained by summing the pre-industrial state (Biotic Equilibrium run) plus the anthropogenic perturbation (abiotic historical minus abiotic equilibrium or control run). For consistency,

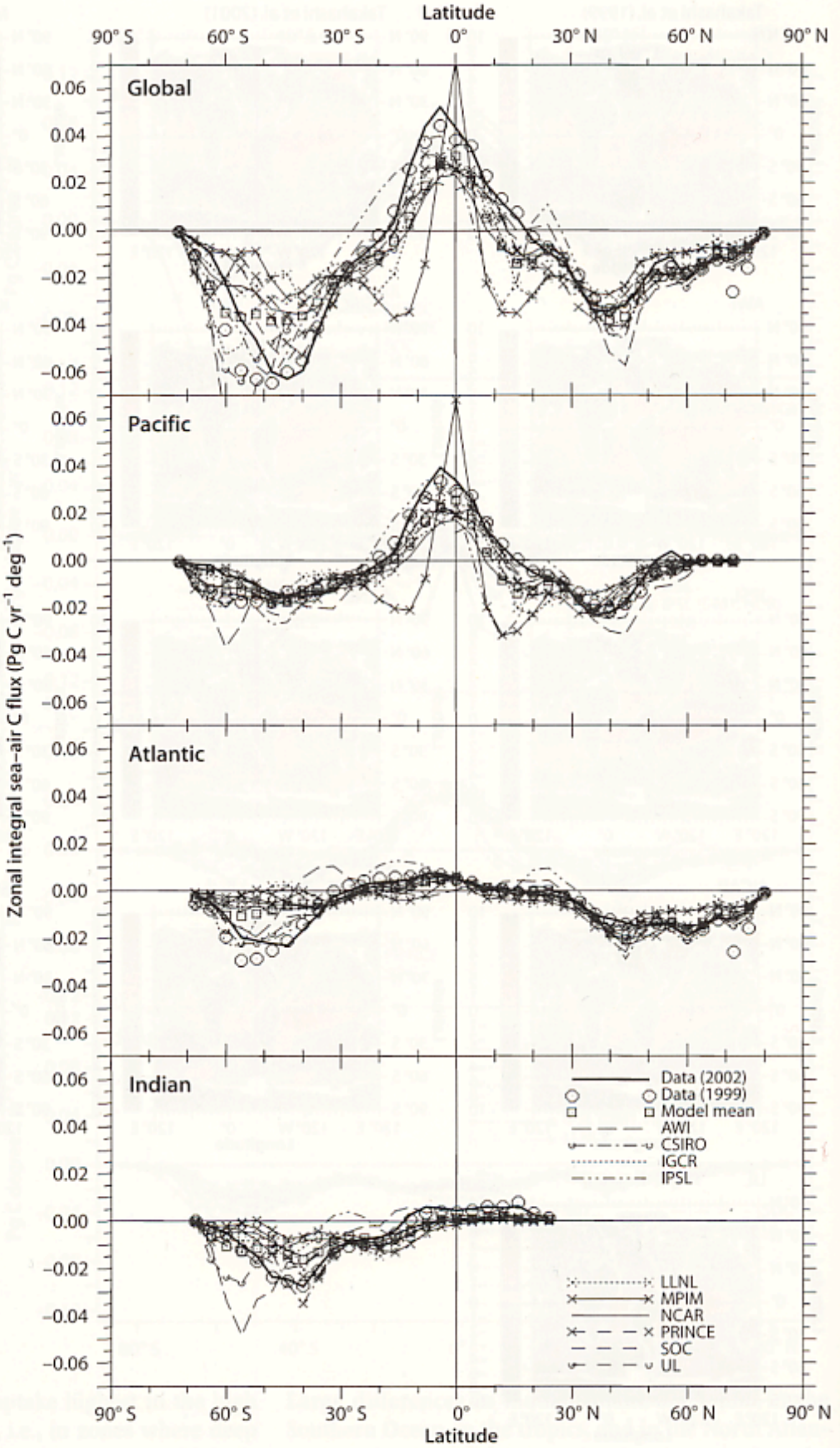

Fig. 5.6.
Zonal integral of the total sea-air CO_2 flux (Fig. 5.5) for the Atlantic, Pacific, and Indian Basins, as well as for the global ocean. The OCMIP-2 models show similar zonally averaged air-sea CO_2 fluxes in the lower latitudes (40° S to 40° N); zonally, models also agree with the data-based estimates. However, modelled air-sea CO_2 fluxes in the Southern Ocean are very different from one another and from the data

models concerning average meridional patterns of storage, as represented by the zonally integrated column inventory. All models store most of the anthropogenic CO_2 in the subtropics (where uptake is lowest), particularly in the southern hemisphere, and they store the least anthropogenic CO_2 in the high latitudes and in the tropics (where uptake is highest). The low storage in these regions results from the surface layer being flushed by subsurface water, low in anthropogenic CO_2, newly entering the mixed layer from below.

Fig. 5.7.
a Zonally integrated, global, cumulative *uptake*, i.e., air-sea flux of anthropogenic CO_2; **b** *storage*, i.e., the inventory of anthropogenic carbon in the ocean (vertical column integral of the concentration), from 1765 to 1995, **c** *convergence* of anthropogenic CO_2 (i.e., storage minus uptake), and **d** northward transport of anthropogenic CO_2

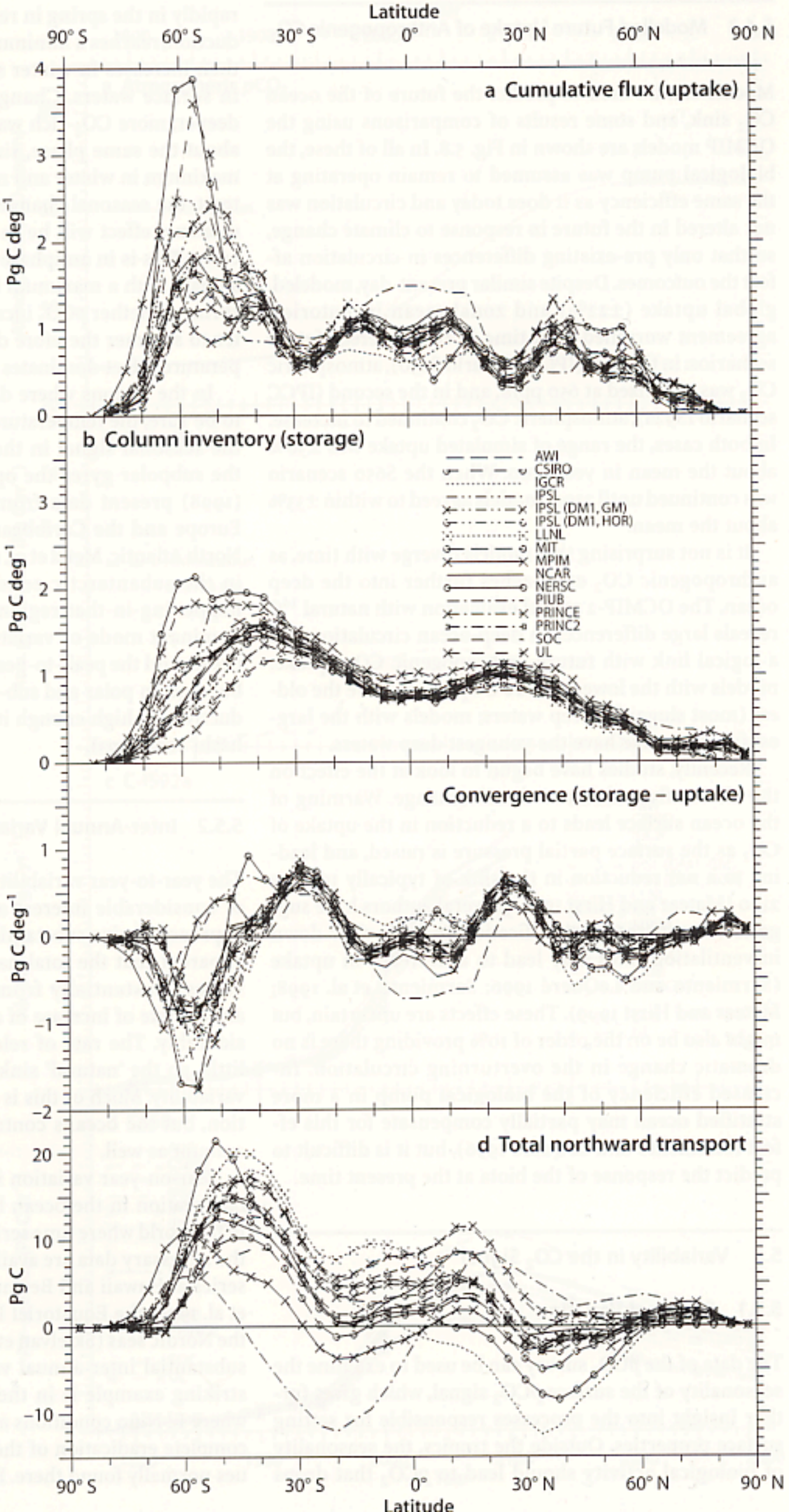

5.4.3 Modelled Future Uptake of Anthropogenic CO_2

Models can be used to predict the future of the ocean CO_2 sink, and some results of comparisons using the OCMIP models are shown in Fig. 5.8. In all of these, the biological pump was assumed to remain operating at the same efficiency as it does today and circulation was not altered in the future in response to climate change, so that only pre-existing differences in circulation affect the outcomes. Despite similar present-day, modeled, global uptake (±22%) and zonal mean inventories, agreement worsened with time in two different future scenarios: in the first (IPCC scenario S650), atmospheric CO_2 was stabilized at 650 ppm, and in the second (IPCC scenario IS92a), atmospheric CO_2 continued to increase. In both cases, the range of simulated uptake was ±30% about the mean in year 2100. When the S650 scenario was continued until 2300, models agreed to within ±33% about the mean.

It is not surprising that models diverge with time, as anthropogenic CO_2 encroaches further into the deep ocean. The OCMIP-2 model evaluation with natural ^{14}C reveals large differences in deep-ocean circulation and a logical link with future anthropogenic CO_2 uptake: models with the lowest future CO_2 uptake have the oldest (most sluggish) deep waters; models with the largest future uptake have the youngest deep waters.

Recently, studies have begun to look at the effect on the air-sea flux of future climate change. Warming of the ocean surface leads to a reduction in the uptake of CO_2 as the surface partial pressure is raised, and leading to a net reduction in the sink of typically 10% by 2100 (Matear and Hirst 1999). Several authors have suggested that increased stratification and/or a slow-down in ventilation rates may lead to a decrease in uptake (Sarmiento and LeQueré 1996; Sarmiento et al. 1998; Matear and Hirst 1999). These effects are uncertain, but might also be on the order of 10% providing there is no dramatic change in the overturning circulation. Increased efficiency of the biological pump in a more stratified ocean may partially compensate for this effect (Sarmiento and LeQueré 1996), but it is difficult to predict the response of the biota at the present time.

5.5 Variability in the CO_2 Signal

5.5.1 Seasonal Variation

The data of the pCO_2 survey can be used to examine the seasonality of the surface pCO_2 signal, which gives further insight into the processes responsible for setting surface properties. Outside the tropics, the seasonality of biological activity should lead to pCO_2 that drops rapidly in the spring in response to maximum net production, reaches a minimum in summer and the fall and then increases in winter as net respiration takes place in surface waters. Changes in the upward mixing of deeper, more CO_2-rich water will produce a cycle with about the same phase, since mixing rates will be at a maximum in winter and minimum in summer. By contrast, the seasonal change in pCO_2 due to the thermodynamic effect will be in phase with the temperature cycle. This is in antiphase to the biological and mixing signals, with a maximum in the fall and a minimum in spring. Whether pCO_2 increases or decreases from winter to summer therefore depends on whether the temperature effect dominates the other two factors.

In the regions where data coverage is good enough to be sure, the temperature effect in general dominates the seasonal signal in the subtropical gyres while in the subpolar gyres the opposite occurs. Cooper et al. (1998) present data from a shipping route between Europe and the Caribbean, showing this effect in the North Atlantic. Metzl et al. (1999) discuss the seasonality in the subantarctic zone and show a similar effect happening in that region. Seasonal variability is the dominant mode of variation over much of the world ocean, and the peak-to-peak magnitude of the cycle can be large. In polar and sub-polar regions where the productivity is high enough it can exceed 100 µatm (Takahashi et al. 1993).

5.5.2 Inter-Annual Variation

The year-to-year variability of the ocean sink is a topic of considerable interest at present, because different approaches give substantially different estimates. It is apparent that the total natural sink, land-plus-ocean, varies substantially from year to year, because the annual rate of increase of atmospheric CO_2 varies considerably. The rate of release from fossil fuel varied little, so the 'natural' sinks must be the cause of this variability. Much of this is caused by terrestrial vegetation, but the oceans contribute an as-yet-unspecified amount as well.

Year-on-year variation is difficult to study by direct observation in the ocean because there are few places in the world where time series have been run. Sites where the necessary data are available include the JGOFS time series at Hawaii and Bermuda (Bates et al. 1996; Sabine et al. 1995) the Equatorial Pacific (Feely et al. 1997) and the Nordic seas (Skjelvan et al. 1999). In all of these sites, substantial inter-annual variability is seen. The most striking example is in the Eastern equatorial Pacific, where El Niño conditions are accompanied by the near-complete eradication of the above-saturation pCO_2 values normally found there. Feely et al. (1997) calculate an

Fig. 5.8.
History of **a** atmospheric CO_2, **b** its growth rate, and the ocean uptake of anthropogenic carbon, under the historical and two future scenarios CIS92a (**c**) and S650 (**d**). All models were forced by observed atmospheric pCO_2 from 1765 to 1990 and subsequently by a concentration scenario chosen by the IPCC for its Third Assessment Report (TAR). The latter scenario is based on the IS92a emissions scenario

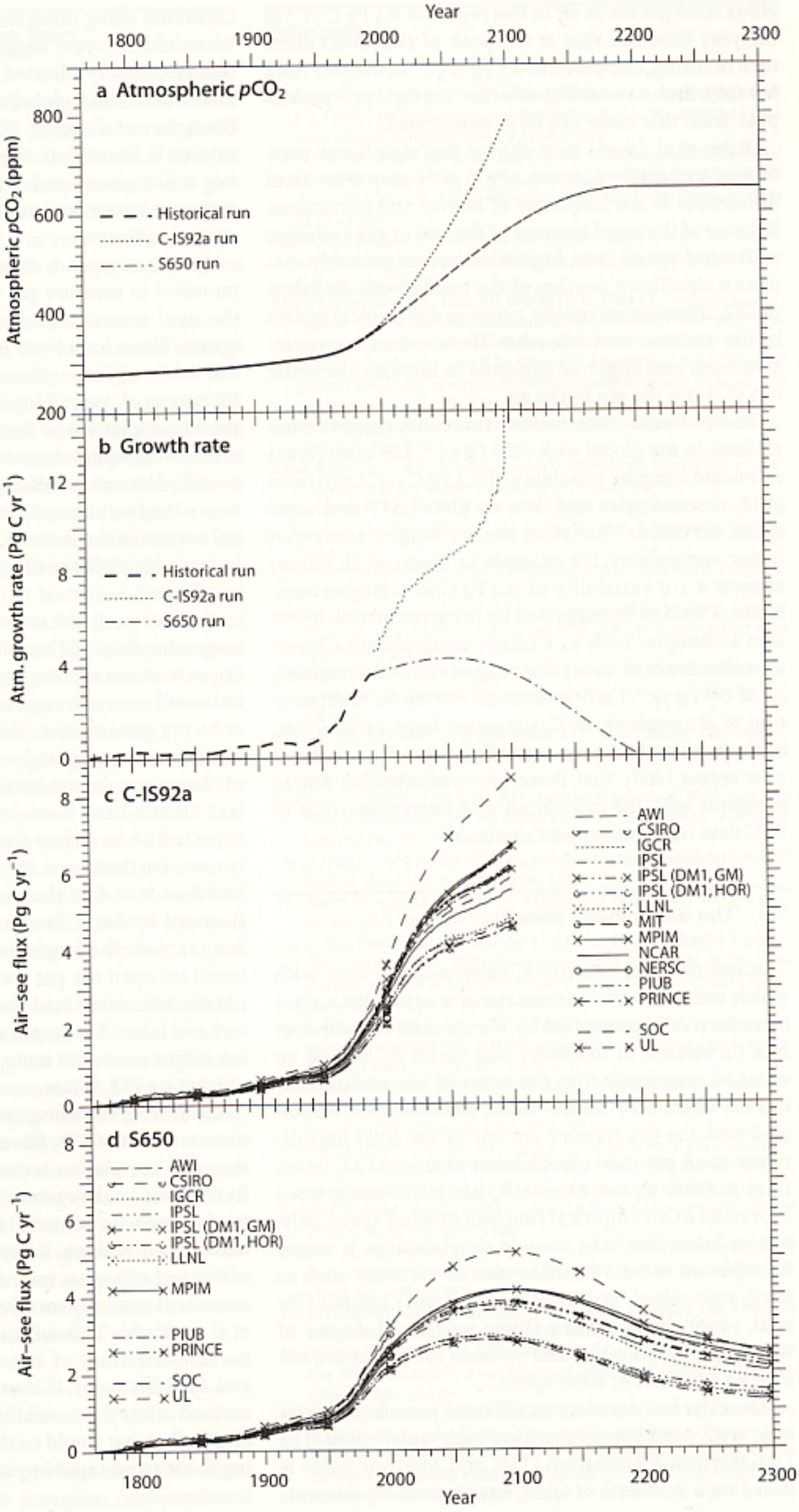

efflux from the sea to air in this region of 0.3 Pg C yr^{-1} in the year from fall 1991 at the peak of the ENSO event then occuring, compared to 0.7 Pg C yr^{-1} in the year from fall 1993, thus a variability of order 0.4 Pg C yr^{-1} peak to peak from this cause can be demonstrated.

Bates et al. (1998) have shown that significant year-to-year variability (i.e., >0.1 Pg C yr^{-1}) may arise from differences in the frequency of storms and hurricanes. Because of the rapid increase of the rate of gas exchange with wind speed, rare, high-wind events probably mediate a significant portion of the total air-sea exchange of CO_2. Hurricanes mostly occur in subtropical waters in late summer and fall, when these waters are supersaturated, and might be expected to increase the efflux of CO_2 from the sea to the air.

In situ ocean observations therefore, suggest variabilities in the global sink ~0.5 Pg yr^{-1}. Lee et al. (1998) estimated a similar variability of 0.4 Pg C yr^{-1} (2-σ) from pCO_2 climatologies and data on global SST and wind speed variations. Modeling studies suggest somewhat larger variabilities, for example Le Queré et al. (2000) suggest a 1-σ variability of 0.4 Pg C yr^{-1}. Higher variabilities tend to be suggested by the atmospheric inversion techniques such as a recent comprehensive inversion (Rayner et al. 1999) that suggests an ocean variability of 0.8 Pg yr^{-1}. Early inversions, relying on interpretation of atmospheric $\delta^{13}C$, suggested large variabilities, of the same order as the mean flux, i.e., 2 Pg yr^{-1}, but it now seems likely that these are overestimates due to problems with the calibration and intercomparison of $\delta^{13}C$ data (R. Francey, pers. comm.).

5.6 The Gas Transfer Velocity

The gas transfer velocity k_v expresses the ease with which molecules of a gas can transfer across the air-sea boundary. It is controlled by the amount of near-surface turbulence in the water and varies by at least an order of magnitude over the range of sea-surface conditions commonly encountered. Uncertainties associated with the gas transfer are one of the chief impediments to an accurate specification of air-sea CO_2 fluxes from oceanic measurements. k_v has traditionally been expressed as an empirical function of wind speed only, but we know this to be a crude simplification. It would be expected to be a function also of variables such as fetch, atmospheric stability (Erickson 1993), rainfall, (Ho et al. 1997), surface films (Frew 1997), and degree of whitecapping (Monhan and Spillane 1984) that are not solely a function of wind speed.

Over the last decade, two different parametrizations of k_v with wind speed have have been widely used. The Liss-Merlivat formulation (Liss and Merlivat 1986) is based on a synthesis of wind-wave tunnel experiments calibrated using observations from a small lake, while Wanninkhof (1992) suggested a simple quadratic function empirically adjusted to be compatible with an estimate of the mean global rate of (^{14}C-based) gas transfer (Broecker et al. 1985). The first of these parameterizations is lower than the second by nearly a factor of two at any given wind speed, creating a substantial uncertainty in any flux estimate based on measurement of partial pressures.

In recent years a number of campaigns have been mounted to measure gas exchange at sea, mostly using the dual tracer method introduced by Watson et al. (1991). These have been interpreted as favoring one or the other of these parameterizations (e.g., compare Watson et al. 1991; Wanninkhof et al. 1993). The most recent compilation of these measurements (Nightingale et al. 2000), updating past treatments, suggests that the overall data set is self-consistent and falls largely between the two parameterizations. There is still substantial scatter in the data set, which can only be explained by introducing factors that do not correlate closely with wind speed.

Further progress must depend on gaining a better understanding of these 'non-wind' factors. Recently, important measurements published by Frew (1997) have indicated a very strong role for natural organic films in reducing gas transfer. These films appear to be much more present in coastal waters than the deep sea. Most of the at-sea determinations of gas transfer over the last decade have been in shelf waters and might be expected to be below the open-ocean values for this reason. Furthermore, the Liss-Merlivat formulation is based on lake data that we might also expect to be influenced by films. Frew's observations may therefore help explain the large discrepancy between estimates based on open sea gas transfer (such as Wanninkhof's parameterization) and those calibrated in coastal waters and lakes. The implication is that the higher, open-sea estimates are the more correct ones to employ when estimating CO_2 fluxes.

Another promising recent development is in the measurement of CO_2 fluxes. Direct measurement using the eddy correlation technique has been used for CO_2 fluxes over land vegetation for decades, but has been too imprecise to be useful for the much lower net fluxes between air and sea. Recently, a careful re-engineering of this technique has improved the precision sufficiently to make at-sea eddy correlation measurements (McGillis et al. 2001a,b). This advance has already enabled new parameterizations of k_v to be suggested (Wanninkhof and McGillis 1999). If it can be reduced to routine, the method offers the possibility of open sea measurements of CO_2 flux that would enable direct testing of the existing theory, and rapid improvements to our CO_2 flux estimates.

5.7 Conclusion: the Next Ten Years

At the conclusion of the JGOFS programme, we have a hugely improved picture of the present state of global ocean fluxes of CO_2 compared to the situation in 1990. We understand in broad terms the processes that give rise to the observed air-sea fluxes, but that understanding is as yet insufficient to make us very confident about predicting how these fluxes will change in the future under a given forcing.

To become confident in our predictions we require a deeper understanding of both the physics and biology of the oceans. In particular, our knowledge of the biological aspects of carbon cycling is largely 'static'; we can describe what happens today, but we are only beginning to understand the processes at the deeper level required to predict how they will change in the future when forced by global change. How, for example, will changes in temperature, pH, circulation and nutrient availability affect the marine biological communities? Will this lead to changes in the efficiency of the biological CO_2 pump? Few models have as yet tried to tackle these issues, and the basic assumption in current use is that the biological parts of the system will not change in the future. To make progress here, we should adopt more laboratory and field investigations targeted at particular processes.

It is clear too that we need ongoing observations, and new types of observations, in order to monitor those processes. The knowledge obtained during JGOFS required an enormous effort by a substantial fraction of the world's marine scientists and marine research resources. Such an effort is unlikely to be repeated for decades to come, so we must develop new methods of observation if we are to maintain and update our understanding in the future.

Fortunately, such techniques are becoming available. For much of the JGOFS decade, no adequate satellite ocean color sensor was flying, but since 1997 high resolution global ocean color coverage has been available. New instruments and techniques for the remote measurement of nutrients, carbon dioxide and fluorescence from drifting and moored buoys and ships of opportunity have been developed (Cooper et al. 1998; Merlivat and Brault 1995; DeGrandpré et al. 1999). We can look forward in the next ten years to a global ocean observing system that will include not only the important physical measurements such as temperature and salinity, but also these vital biogeochemical variables.

Acknowledgements

This work was supported by contract no. EVK2-2000-22058 (CAVASSOO) from the European commission.

References

Aumont O, Orr JC, Monfray P, Ludwig W, Amiotte-Suchet P, Probst J-L (2001) Riverine-driven interhemispheric transport of carbon. Global Biogeochem Cy 15:393–405

Bates NR, Michaels AF, Knap AH (1996) Seasonal and interannual variability of oceanic carbon dioxide species at the US JGOFS Bermuda Atlantic Time-series Study (BATS) site. Deep-Sea Res Pt II 43:347–383

Bates NR, Knap AH, Michaels AF (1998) Contribution of hurricanes to local and global estimates of air-sea exchange of CO_2. Nature 395:58–61

Battle M, Bender ML, Tans PP, White JWC, Ellis JT, Conway T, et al. (2000) Global carbon sinks and their variability inferred from atmospheric O_2 and $\delta^{13}C$. Science 287:2467–2470

Bousquet P, Peylin P, Ciais P, Le Queré C, Friedlingstein P, Tans PP (2000) Regional changes in carbon dioxide fluxes of land and oceans since 1980. Science 290:1342–1346

Brewer PG (1978) Direct measurement of the oceanic CO_2 increase. Geophys Res Lett 5:997–1000

Broecker WS, Peng TH (1992) Interhemispheric transport of carbon-dioxide by ocean circulation. Nature 356:587–589

Broecker WS, Peng TH, Ostlund G, Stuiver M (1985) The distribution of bomb radiocarbon in the ocean. J Geophys Res 90: 6953–6970

Chen C-T, Millero FJ (1979) Gradual increase of oceanic CO_2. Nature 277:205–206

Ciais P, Peylin P, Bousquet P (2000) Regional biospheric carbon fluxes as inferred from atmospheric CO_2 measurements. Ecol Appl 10:1574–1589

Conway TJ, Tans PP (1999) Development of the CO_2 latitude gradient in recent decades. Global Biogeochem Cy 13: 821–826

Cooper DJ, Watson AJ, Nightingale PD (1996) Large decrease in ocean-surface CO_2 fugacity in response to in-situ iron fertilization. Nature 383:511–513

Cooper DJ, Watson AJ, Ling RD (1998) Variation of pCO_2 along a North Atlantic shipping route (UK to Caribbean): a year of automated observations. Mar Chem 60:147–164

DeGrandpré MD, Baehr MM, Hammar TR (1999) Calibration-free opitcal chemical sensors. Anal Chem 71:1152–1159

Erickson DJ (1993) A stability dependent theory for air-sea gas-exchange. J Geophys Res 98:8471–8488

Feely RA, Wanninkhof R, Goyet C, Archer DE, Takahashi T (1997) Variability of CO_2 distributions and sea-air fluxes in the central and eastern equatorial Pacific during the 1991–1994 El Niño. Deep-Sea Res Pt II 44:1851–1867

Feely RA, Sabine CL, Keys RM, Peng T-H (1999) CO_2 synthesis results: estimating the anthropgenic carbon dioxide sink in the Pacific Ocean. US JGOFS News 9:1–5

Fitzwater SE, Coale KH, Gordon RM, Johnson KS, Ondrusek ME (1996) Iron-deficiency and phytoplankton growth in the Equatorial Pacific. Deep-Sea Res Pt II 43:995–1015

Frew NM (1997) The role of organic films in air-sea gas exchange. In: Liss PS, Duce RA (eds) The sea surface and global change. Cambridge University Press, Cambridge, pp 121–171

Gruber N (1998) Anthropogenic CO_2 in the Atlantic Ocean. Global Biogeochem Cy 12:165–191

Gruber N, Sarmiento JL, Stocker TF (1996) An improved method for detecting anthropogenic CO_2 in the oceans. Global Biogeochem Cy 10:809–837

Ho DT, Bliven LF, Wanninkhof R, Schlosser P (1997) The effect of rain on air-water gas exchange. Tellus B 49:149–158

Houghton JT, Jenkins GJ, Ephraums JJ (eds) (1990) Climate change: the IPCC scientific assessment. Cambridge University Press, Cambridge, 364 pp

Houghton JT, Meira Filho LG, Callendar BA, Harris N, Kattenberg A, Maskell K (eds) (1995) The science of climate change: contribution of Working Group I to the second assessment of the Intergovernmental Panel on Climate Change. Cambridge University Press, Cambridge, 572 pp

Houghton JT, Ding Y, Griggs DJ, Noguer M, van der Linden PJ, Xiaosu D (eds) (2001) Climate change 2001: the scientific basis contribution of Working Group I to the third assessment report of the Intergovernmental Panel on Climate Change. Cambridge University Press, Cambridge, 944 pp

Indermuhle A, Stocker TF, Joos F, Fischer H, Smith HJ, Wahlen M, et al. (1999) Holocene carbon-cycle dynamics based on CO_2 trapped in ice at Taylor Dome, Antarctica. Nature 398:121–126

Kaminski T, Heimann M, Giering R (1999) A coarse grid three-dimensional global inverse model of the atmospheric transport – 2. Inversion of the transport of CO_2 in the 1980s. J Geophys Res 104:18555–18581

Keeling CD, Bacastow RB, Carter AF, Piper SC, Whorf TP, Heimann M, et al. (1989) A three-dimensional model of atmospheric CO_2 transport based on observed winds. 1. Analysis of observational data. In: Peterson DH (ed) Aspects of climate variability in the Pacific and the Western Americas Geophysical Monograph. American Geophysical Union, 55, 165–235

Keeling RF, Peng TH (1995) Transport of heat, CO_2 and O_2 by the Atlantic's thermohaline circulation. Philos T Roy Soc B 348: 133–142

Keeling RF, Shertz SR (1992) Seasonal and interannual variations in atmospheric oxygen and implications for the global carbon cycle. Nature 358:723–727

Keeling RF, Piper SC, Heimann M (1996) Global and hemispheric CO_2 sinks deduced from changes in atmospheric O_2 concentration. Nature 381:218–221

Kheshgi HS, Jain AK, Wuebbles DJ (1999) Model-based estimation of the global carbon budget and its uncertainty from carbon dioxide and carbon isotope records. J Geophys Res 104: 31127–31143

Langenfelds RL, Francey RJ, Steele LP, Battle M, Keeling RF, Budd WF (1999) Partitioning of the global fossil CO_2 sink using a 19-year trend in atmospheric O_2. Geophys Res Lett 26:1897–1900

Le Quere C, Orr JC, Monfray P, Aumont O, Madec G (2000) Interannual variability of the oceanic sink of CO_2 from 1979 through 1997. Global Biogeochem Cy 14:1247–1265

Lee K, Wanninkhof R, Takahashi T, Doney SC, Feely RA (1998) Low interannual variability in recent oceanic uptake of atmospheric carbon dioxide. Nature 396:155–159

Lefevre N, Watson AJ, Cooper DJ, Weiss RF, Takahashi T, Sutherland SC (1999) Assessing the seasonality of the oceanic sink for CO_2 in the northern hemisphere. Global Biogeochem Cy 13:273–286

Lerperger M, McNichol AP, Peden J, Gagnon AR, Elder KL, Kutschera W, et al. (2000) Oceanic uptake of CO_2 re-estimated through $\delta^{13}C$ in WOCE samples. Nucl Instrum Meth B 172: 501–512

Li XS, Berger A, Loutre MF (1998) CO_2 and northern hemisphere ice volume variations over the middle and late quaternary. Clim Dynam 14:537–544

Liss PS, Merlivat L (1986) Air-sea gas exchange rates: introduction and synthesis. In: Buat-Menard P (ed) The role of air-sea exchange in geochemical cycling. D. Reidel, Dordrecht, pp 113–127

Ludwig W, Amiotte-Suchet P, Munhoven G, Probst JL (1998) Atmospheric CO_2 consumption by continental erosion: present-day controls and implications for the last glacial maximum. Global Planet Change 17:107–120

Matear RJ, Hirst AC (1999) Climate change feeback on the future oceanic CO_2 uptake. Tellus B 51:722–733

McGillis WR, Edson JE, Hare JE, Fairall CW (2001a) Direct covariance air-sea CO_2 fluxes. J Geophys Res 106:16729–16745

McGillis WR, Edson JB, Ware JD, Dacey JWH, Hare JE, Fairall CW, Wanninkhof R (2001b) Carbon dioxide flux techniques performed during GasEx 98. Mar Chem 75:267–280

McKinley GA, Follows MJ, Marshall J (2000) Interannual variability in the air-sea flux of oxygen in the North Atlantic. Geophys Res Lett 27:2933–2936

Merlivat L, Brault P (1995) CARIOCA buoy, carbon dioxide monitor. Sea Technol 10:23–30

Metzl N, Tilbrook B, Poisson A (1999) The annual fCO_2 cycle and the air-sea CO_2 flux in the sub-Antarctic Ocean. Tellus B 51: 849–861

Monahan EC, Spillane MC (1984) The role of oceanic whitecaps in air-sea gas exchange. In: Brutaert W, Jirka GH (eds) Gas transfer at water surfaces. D. Reidel, Dordrecht, pp 495–504

Murray JW, Barber RT, Roman MR, Bacon MP, Feely RA (1994) Physical and biological controls on carbon cycling in the Equatorial Pacific. Science 266:58–65

Nightingale PD, Malin G, Law CS, Watson AJ, Liss PS, Liddicoat MI, et al. (2000) In situ evaluation of air-sea gas exchange parameterizations using novel conservative and volatile tracers. Global Biogeochem Cy 14:373–387

Orr JC (1993) Accord between ocean models predicting uptake of anthropogenic CO_2. Water Air Soil Poll 70:465–481

Orr JC, Maier-Reimer E, Mikolajewicz U, Monfray P, Sarmiento JL, Toggweiler JR, et al. (2001) Estimates of anthropogenic carbon uptake from four three-dimensional global ocean models. Global Biogeochem Cy 15:43–60

Ostlund HG, Possnert G, Swift JH (1987) Ventilation rate of the deep Arctic Ocean from ^{14}C-data. J Geophys Res 92:3769–3777

Pearman GI, Hyson P (1986) Global transport and inter-reservoir exchange of carbon dioxide with particular reference to stable isotope distributions. J Atmos Chem 4:81–124

Quay PD, Tilbrook B, Wong CS (1992) Oceanic uptake of fossil-fuel CO_2: ^{13}C evidence. Science 256:74–79

Rayner PJ, Law RM, Dargaville R (1999) The relationship between tropical CO_2 fluxes and the El Niño-Southern Oscillation. Geophys Res Lett 26:493–496

Sabine CL, Mackenzie FT, Winn C, Karl DM (1995) Geochemistry of carbon dioxide in seawater at the Hawaii Ocean Time-Series Station, Aloha. Global Biogeochem Cy 9:637–651

Sabine CL, Key RM, Johnson KM, Millero FJ, Poisson A, Sarmiento JL, et al. (1999) Anthropogenic CO_2 inventory in the Indian Ocean. Global Biogeochem Cy 13:179–198

Sabine CL, Wanninkhof R, Key RM, Goyet C, Millero FJ (2000) Seasonal CO_2 fluxes in the tropical and subtropical Indian Ocean. Mar Chem 72:33–53

Sarmiento JL, Le Quere C (1996) Oceanic carbon dioxide uptake in a model of century-scale global warming. Science 274: 1346–1350

Sarmiento JL, Sundquist ET (1992) Revised budget for the oceanic uptake of anthropogenic carbon-dioxide. Nature 356:589–593

Sarmiento JL, Toggweiler JR (1984) A new model for the role of the oceans in determining atmospheric pCO_2. Nature 308:621–624

Sarmiento JL, Toggweiler JR, Najjar R (1988) Ocean carbon-cycle dynamics and atmospheric pCO_2. Philos Tr R Soc S-A 325:3–21

Sarmiento JL, Hughes TMC, Stouffer RJ, Manabe S (1998) Simulated response of the ocean carbon cycle to anthropogenic climate warming. Nature 393:245–249.

Sarmiento JL, Monfray P, Maier-Reimer E, Aumont O, Murnane RJ, Orr JC (2000) Sea-air CO_2 fluxes and carbon transport: a comparison of three ocean general circulation models. Global Biogeochem Cy 14:1267–1281

Shackleton NJ (2000) The 100 000-year ice-age cycle identified and found to lag temperature, carbon dioxide, and orbital eccentricity. Science 289:1897–1902

Siegenthaler U, Joos F (1992) Use of a simple model for studying oceanic tracer distributions and the global carbon cycle. Tellus B 44:186–207

Siegenthaler U, Sarmiento JL (1993) Atmospheric carbon-dioxide and the ocean. Nature 365:119–125

Skjelvan I, Johannessen T, Miller LA (1999) Interannual variability of fCO_2 in the Greenland and Norwegian Seas. Tellus B 51:477–489

Sonnerup RE, Quay PD, McNichol AP, Bullister JL, Westby TA, Anderson HL (1999) Reconstructing the oceanic ^{13}C Suess effect. Global Biogeochem Cy 13:857–872

Sundquist ET (1985) Geological perspectives on carbon dioxide and the carbon cycle. In: Sundquist ET, Broecker WS (eds) The carbon cycle and atmospheric CO_2: natural variations archean to present. American Geophysical Union, Washington D.C., pp 5–69

Takahashi T, Olafsson J, Goddard JG, Chipman DW, Sutherland SC (1993) Seasonal-variation of CO_2 and nutrients in the high-latitude surface oceans – a comparative study. Global Biogeo-

Takahashi T, Feely RA, Weiss RF, Wanninkhof RH, Chipman DW, Sutherland SC, et al. (1997) Global air-sea flux of CO_2: an estimate based on measurements of sea-air pCO_2 difference. P Natl Acad Sci Usa 94:8292–8299

Takahashi T, Wanninkhof RH, Feely RA, Weiss RF, Chipman DW, Bates N, et al. (1999) Net sea-air CO_2 flux over the global oceans: an improved estimate based on the sea-air pCO_2 difference. In: Nojiri Y (ed) Proceedings of the 2nd Internations Symposium on CO_2 in the Oceans, Tsukuba, January 1999. National Institute for Environmental studies, Tsukuba, Japan, pp 9–15

Takahashi T, Sutherland SC, Sweeney C, Poisson A, Metzl N, Tilbrook B, Bates N, Wanninkhof R, Feely RA, Sabine C, Olafsson J, Nojiri Y (2002) Global sea-air CO_2 flux based on climatological surface ocean pCO_2, and seasonal biological and temperature effects. Deep-Sea Res Pt II 49:1601–1622

Taylor JA, Orr JC (2000) The natural latitudinal distribution of atmospheric CO_2. Global Planet Change 26:375–386

Torres R, Turner DR, Silva N, Rutllant J (1999) High short-term variability of CO_2 fluxes during an upwelling event off the Chilean coast at 30° S. Deep-Sea Res Pt I 46:1161–1179

Wanninkhof R (1992) Relationship between wind speed and gas exchange over the ocean. J Geophys Res 97:7373–7382

Wanninkhof R, McGillis WR (1999) A cubic relationship between air-sea CO_2 exchange and wind speed. Geophys Res Lett 26:1889–1892

Wanninkhof R, Asher W, Weppernig R, Chen H, Schlosser P, Langdon C, et al. (1993) Gas transfer experiment on Georges Bank using 2 volatile deliberate tracers. J Geophys Res 98:20237–20248

Watson AJ, Liss PS (1998) Marine biological controls on climate via the carbon and sulphur geochemical cycles. Philos T Roy Soc B 353:41–51

Watson AJ, Upstill-Goddard RC, Liss PS (1991) Air sea gas-exchange in rough and stormy seas measured by a dual-tracer technique. Nature 349:145–147

Weiss RF (1974) Carbon dioxide in water and sea water; the solubility of a non-ideal gas. Mar Chem 2:203–215